

May 2012

# Mitigation of the LHC Inverse Problem

NICKI BORNHAUSER<sup>1</sup> AND MANUEL DREES<sup>1</sup>

<sup>1</sup>*Physikalisches Institut and Bethe Center for Theoretical Physics, Universität Bonn, Nußallee  
12, D-53115 Bonn, Germany*

## Abstract

The LHC inverse problem refers to the difficulties in determining the parameters of an underlying theory from data (to be) taken by the LHC experiments: if they find signals of new physics, and an underlying theory is assumed, could its parameters be determined uniquely, or do different parameter choices give indistinguishable experimental signatures? This inverse problem was studied before for a supersymmetric Standard Model with 15 free parameters. This earlier study found 283 indistinguishable pairs of parameter choices, called degenerate pairs, even if backgrounds are ignored. We can resolve all but 23 of those pairs by constructing a true  $\chi^2$  distribution using mostly counting observables. The elimination of systematic errors would even allow separating the residual degeneracies. Taking the Standard Model background into account we still can resolve 237 of the 283 “degenerate” pairs. This indicates that (some of) our observables should also be useful for the purpose of determining the values of SUSY parameters.

arXiv:1205.6080v2 [hep-ph] 3 Jul 2012

# 1 Introduction

The Large Hadron Collider (LHC) is successfully running and collecting data. It is hoped that in the near future signs of “new physics” will show up. Once a signal for physics beyond the Standard Model (SM) has been established, one would need to identify the underlying theory, and to determine its parameters. For a given theory in an ideal world a certain parameter choice would lead to a unique experimental signature. In this case the “inverse problem”, of going from experimental observables to parameters of the underlying theory, would have a unique solution. However, it is quite possible that – even within a given theory – several different sets of parameters reproduce all observables that are available at a given time. Note that we are here not concerned about (small) regions of parameter space centered around the true solution; it is clear that in the presence of non-vanishing experimental errors, a finite region of parameter space will be allowed even if the inverse problem does have a unique solution. Rather, the concern is that quite different, not necessarily connected regions of parameter space cannot be disentangled using only (future) LHC data.

This issue has been studied in most detail in the framework of the minimal supersymmetric extension of the SM, the MSSM [1]. Most studies focused on determining the masses of specific sparticles using features of kinematic distributions, including invariant mass “edges” [2] or “kinks” in more complicated observables [3]. This uses only kinematical information, and ideally allows to directly determine the masses of the involved superparticles. These can then be compared to predictions of specific models of supersymmetry breaking, or to fix the parameters of such models. The model dependence thus enters only at the last stage of the analysis.

One disadvantage of these kinematical methods is that dynamical information, i.e. information on counting rates which determine products of cross sections and branching ratios, is not used at all. It has been realized quite early that (ratios of) numbers of events of specific types can be used to discriminate between variants of the MSSM [4,5]. More recently, information on the total event rate after cuts has been shown to improve the performance of purely kinematical fits [6]. Even in that case this method has generally only been used in constrained versions of the MSSM, with a rather small number of free parameters. This allows to focus on the most prominent kinematical features, since only a small number of masses needs to be measured in order to determine all free parameters of the theory.

Another disadvantage of parameter reconstruction based on kinematic edges or kinks is that it is not straightforward to automatize them. Generally human intervention is required to detect an edge. This method is therefore well suited to detailed analyses of benchmark points (and eventually of real data, it is hoped), but cannot easily be used for broad scans of parameter space.

In order to overcome the last two disadvantages, Arkani-Hamed *et. al.* [7] attempted a “brute-force” approach to the parameter reconstruction issue in the context of a quite general version of the MSSM with 15 free parameters defined at the weak (or superparticle mass) scale.\* They randomly generated 43,026 sets of parameters, called “models” by them. For each parameter set they Monte Carlo generated the number of events corresponding to an integrated luminosity of  $10 \text{ fb}^{-1}$  at a center of mass energy of 14 TeV. They analyzed these events using a

---

\* A fully general MSSM has many more free parameters. However, most of those are related to flavor mixing and/or CP violation, and are strongly constrained by low-energy observables and/or have little influence on collider phenomenology.

total of 1808 observables. Most of them are kinematical observables (based on invariant mass and transverse momentum distributions<sup>†</sup>); less than ten percent of the observables are counting observables (number of events with a certain property). Based on a statistical analysis, 283 so-called degenerate model pairs were identified. These are pairs of parameter sets that could not be distinguished by their method of comparison with an estimated 95% confidence level [7].

Note that the analysis of ref. [7] used a very large number of observables, but was still unable to distinguish between even quite different spectra, even though the sparticle mass scale did not exceed 1 TeV. This can be interpreted as implying that the LHC experiments are in principle incapable of determining all MSSM parameters in a model-independent fashion.

However, the analysis of ref. [7] has several weaknesses. To begin with, initial state radiation and the “underlying event” (thought to arise from interactions between the “spectator partons” not taking part in the primary hard interaction) are ignored. These features enlarge the event; since they do not depend much on the produced final state, they can be expected to reduce the observable differences between different parameter sets even more, i.e. to increase the number of degenerate pairs.

Another criticism is that Arkani-Hamed *et al.* use a single “ $\chi^2$ -like” quantity, called  $(\Delta S_{AB})^2$ , to analyze the information of all 1808 observables; here  $A, B$  stand for two sets of parameters, and  $(\Delta S_{AB})^2$  essentially sums the squared differences between the predicted observables, divided by the squared total error of these observables, and normalized to the number of observables included. An observable is included in the definition of  $(\Delta S_{AB})^2$  only if the total error is smaller than both predictions or smaller than the difference between the predictions; this is meant to reduce the dilution of  $(\Delta S_{AB})^2$  by observables that are so poorly measured that they cannot discriminate between parameter sets.

Nevertheless the dilution of the statistical measure by observables with little discriminatory power remains an issue. In fact, Arkani-Hamed *et al.* found [7] that 46 out of the 283 “degenerate” pairs had (at least) one observable differing by more than 5 estimated standard deviations, even if one only considers the subset of observables constructed from final states containing two charged leptons. They do not consider this to be significant, since when comparing 2,600 parameter sets with themselves, but run with different seed of the Monte Carlo event generator, they found 611 cases where (at least) one di-lepton observable differed by more than five estimated standard deviations between the two runs.

This example casts serious doubt on the estimate of the standard deviation of  $(\Delta S_{AB})^2$  used in ref. [7]. Recall that for a normal (Gaussian) distributed observable, the probability of two measurements to differ by more than five (true) standard deviations is about  $5.7 \cdot 10^{-7}$ . By our count Arkani-Hamed *et al.* include around 1,000 di-lepton observables. Even if they were all statistically independent, one would expect at most  $5.7 \cdot 10^{-7} \times 1000 \times 2600 \approx 1.5$  observables to differ at more than five standard deviations. Since the observables used in ref. [7] are actually highly correlated, as acknowledged by Arkani-Hamed *et al.*, the number of statistically independent di-lepton observables is much smaller than 1,000, reducing the probability to observe true  $5\sigma$  fluctuations even more. The fact that 611 such fluctuations were observed thus indicates a problem with the estimate of the error and/or with the generation of the events.

---

<sup>†</sup> Rather than looking for edges or kinks in these distributions, they bin them in ten or 20 bins, such that each bin contains the same number of events. The observables are then the boundaries of these bins. These observables can obviously be constructed automatically, without human intervention.

A possibly related issue is that the correlations between observables are not included in the definition of  $(\Delta S_{AB})^2$  [7]; this is why this quantity is a “ $\chi^2$ -like” variable, rather than a true  $\chi^2$ . This means that the statistical interpretation of this observable is not a priori clear. Arkani-Hamed et al. address this problem by again comparing parameter sets to themselves, generated with different seeds of the random number generator. They found that in 5% of all cases  $(\Delta S_{AB})^2 > 0.285$  even for the same parameter set. They therefore defined  $(\Delta S_{AB})^2 > 0.285$  as equivalent to two sets of parameters being distinguishable at 95% confidence level. This inference is not obvious to us, since the statistical properties of  $(\Delta S_{AB})^2$  are a priori unknown, and the comparison of parameter sets with themselves yielded results that seem violently at odds with the usual interpretation in terms of standard deviations.

Finally, the variable  $(\Delta S_{AB})^2$  is constructed to resemble a  $\chi^2$  comparing two different measurements, both of which are assigned the statistical uncertainties expected for a data sample of  $10 \text{ fb}^{-1}$ . However, the issue is whether, given that Nature chose parameter set A, a measurement can exclude the *prediction* made for parameter set B. This prediction should (in principle) have negligible statistical uncertainty. It is not clear to what extent this distorts the statistics, since the cut-off for  $(\Delta S_{AB})^2$  that defines which pairs are deemed indistinguishable is determined by Monte Carlo experiments; however, conceptually there is a significant difference between comparing two experiments and comparing an experiment with a prediction.

In this paper we re-analyze the degenerate pairs of ref. [7]; for statistical tests we also employ a larger sample of pairs with slightly larger  $(\Delta S_{AB})^2$ . We include initial-state radiation as well as the underlying event, and analyze events at the hadron level. We want to construct a true  $\chi^2$ , in order to have an observable with well-defined statistical properties. Moreover, we focus on counting signatures. One reason for this is that it is relatively easy to define statistically independent counting rates, by simply defining mutually exclusive classes of events. In contrast, since all events of a given class contribute to various kinematical observables, these observables will be statistically correlated. A second reason is that there is a much larger literature on using kinematical quantities [2,3] than on the use of counting rates [4–6]. Here we want to show that counting rates can play an important role in discriminating between sets of MSSM parameters; we view this as a first step towards a determination of the values of these parameters, including statistically meaningful errors. Altogether we employ (at most) 84 observables when comparing sets of parameters. Since most of these observables are counting rates, which should not depend sensitively on details of the detectors, we do not use a detector simulation (unlike ref. [7]); however, we use realistic efficiencies when counting  $b$ -jets and  $\tau$ -leptons. Moreover, unlike ref. [7] we also investigate the effect of SM backgrounds.

The remainder of this article is organized as follows. In the next Section we describe the definition of the sets of parameters, as well as some technical details of our simulation. In Sec. 3 we list the observables we use, and construct an overall  $\chi^2$  variable out of them. We perform some checks to show that this variable has the desired statistical properties. Section 4 contains the results of our numerical analysis, and we conclude in Sec. 5. Details of the definition of objects (jets, leptons) and of the cuts employed are given in the Appendices.

## 2 The Simulation

In this Section we give some details of our simulation. We start with a description of how the sets of MSSM parameters were chosen in ref. [7], and then describe how we generate events.

### 2.1 Parameter Sets

Here we follow ref. [7]. There the MSSM spectrum was parameterized directly at the superparticle mass scale, using the following 15 free parameters: three gaugino masses  $M_1$  (bino),  $M_2$  (wino) and  $M_3$  (gluino); four independent slepton masses  $m_{\tilde{e}_L} = m_{\tilde{\mu}_L}$ ,  $m_{\tilde{e}_R} = m_{\tilde{\mu}_R}$ ,  $m_{\tilde{\tau}_L}$  and  $m_{\tilde{\tau}_R}$ ; six independent squark masses  $m_{\tilde{q}_{1L}} = m_{\tilde{q}_{2L}}$ ,  $m_{\tilde{q}_{3L}}$ ,  $m_{\tilde{u}_R} = m_{\tilde{c}_R}$ ,  $m_{\tilde{t}_R}$ ,  $m_{\tilde{d}_R} = m_{\tilde{s}_R}$  and  $m_{\tilde{b}_R}$ ; the Higgs(ino) mass parameter  $\mu$ ; and the ratio of vacuum expectation values  $\tan\beta$ . The masses of the first and second generation sfermions with given quantum numbers are taken equal; this automatically satisfies stringent constraints on flavor changing neutral currents in this sector [1]. Four additional parameters are fixed, namely the trilinear scalar couplings  $A_t = A_b = A_\tau = 800$  GeV and the pseudoscalar Higgs pole mass  $m_A = 850$  GeV. Out of the  $A$ -parameters, only  $A_t$  is expected to have significant influence on LHC phenomenology in the context of the MSSM, but determining its parameters is expected to be quite difficult. Fixing its value therefore reduces the difficulty of the overall problem. Similarly, determining  $m_A$  is likely quite difficult, unless it is so small that the heavy Higgs bosons can be produced abundantly.

43,026 sets of parameters were then generated in [7], by randomly choosing values of the free parameters, with probability distributions that are flat within certain ranges. In particular, the parameters  $M_1$ ,  $M_2$  and  $\mu$  and the four slepton masses lie between 100 GeV and 1 TeV. The gluino mass and the six squark masses lie between 600 GeV and 1 TeV,<sup>‡</sup> and  $\tan\beta$  varies between 2 and 50. The relations between the parameters are further restricted by the condition

$$m_{\text{slepton}}^{\text{max}} < m_{\text{ewino}}^{\text{max}} + 50 \text{ GeV} < m_{\text{color}}^{\text{max}} + 100 \text{ GeV}, \quad (2.1)$$

with  $m_{\text{slepton}}^{\text{max}}$  being the maximum slepton soft mass,  $m_{\text{ewino}}^{\text{max}}$  being the maximum of  $M_1$ ,  $M_2$  and  $\mu$ , and  $m_{\text{color}}^{\text{max}}$  being the maximum soft mass or mass parameter of any color-charged superparticle. The constraints (2.1) can be motivated by the fact that most models of supersymmetry breaking predict [1] superparticles with non-vanishing color charge to be heavier than the color singlets. They also make it likely [7] that sleptons can be produced in the decay of some color-charged superparticle, improving the chance that slepton masses can be determined experimentally.

### 2.2 Event Generation

Given the parameters of the (weak-scale) MSSM Lagrangian, we compute the supersymmetric spectrum with the program SOFTSUSY [9]. Next, the branching ratios of kinematically allowed decays are computed using SUSY-HIT [10]. Signal events are then generated with the event generator Herwig++ [11]. We first generate 10,000 events to determine the total cross section for the production of superparticles, and then generate the number of events corresponding to

---

<sup>‡</sup> This means that many of the scenarios considered in ref. [7] are likely excluded by published analyses of LHC data [8]. We nevertheless use the same parameter sets in order to be able to directly compare our analysis with the results of ref. [7].

an integrated luminosity of  $10 \text{ fb}^{-1}$  of data at  $\sqrt{s} = 14 \text{ TeV}$ . We include full QCD showering as well as interactions between spectator partons, using default values of the corresponding parameters. Since all cross sections are calculated in leading order (LO) in QCD, we use LO parton distribution functions CTEQ6.6 [12].

We do not attempt any detailed detector modeling. We do not expect experimental resolutions to be very important for us, since most of the observables we employ are counting observables, which should be relatively insensitive to resolution effects. Acceptances (both in pseudorapidity and transverse momentum) are included in our definitions of observable leptons and jets, as described in Appendix A. Moreover, we assume that hadronically decaying  $\tau$ -leptons as well as  $b$ -jets can be tagged with 50% probability within their respective acceptance windows. We do not include false positive tags. Within the MSSM, all flavors of quarks and leptons are produced with comparable probabilities, so mis-tagging is not likely to significantly affect the distinction between different parameter sets, which is at the focus of our analysis.

### 3 Method of Comparing Parameter Sets

In this section we describe how we compare parameter sets. To this end we construct a total  $\chi^2$  distribution, which allows us to compute a  $p$ -value, which in turn is used to quantify how similar two parameter sets appear. This is described in the last Subsection. The first Subsection discusses the observables we use to construct the overall  $\chi^2$ , and the second Subsection describes the calculation of the covariance matrix for these observables.

#### 3.1 Observables

If two different parameter choices yield exactly the same values for all conceivable observables, then there would be no chance to distinguish between these parameter sets. In principle this should not happen for the 15 parameter MSSM we are considering, since each parameter affects the mass, production cross section and/or decay branching ratios of at least one superparticle. However, while masses, cross sections and branching ratios formally are all observables, it is not clear whether they affect quantities that can actually be measured by LHC experiments sufficiently strongly to allow determination of the corresponding parameters from LHC data. Moreover, it is possible that the values of two or more parameters can be varied simultaneously such that no LHC observable is changed significantly.

Choosing the right set of observables is a quite non-trivial task. On general grounds one expects that one needs at least one observable for each free parameter whose value one wishes to determine.\* Supersymmetric extensions of the SM are notorious for allowing many possible signatures [1]; however, not all signatures are viable for all combinations of parameters. This argues for using not too few observables, in order to make sure that one is sensitive to all parameters everywhere in parameter space.

---

\* This is not strictly true. If some observable happens to take its absolute minimum or maximum, it alone would suffice to determine all free parameters. In practice this is not likely to happen for a simple observable (a counting rate or kinematical observable for a given final state).

Conversely, an observable should show non-trivial dependence on at least one of the free parameters in order to be useful. If we combine all observables into a single quantity, adding observables with little or no discriminatory power can dilute the effect of those observables that are sensitive to some parameters, reducing the statistical power of the test.

Another argument against simply using “all” observables, as (essentially) done by Arkani-Hamed et al. [7], is that this makes it difficult to determine a priori the statistical correlations between the observables. Since our method of comparing parameter sets is based on an overall  $\chi^2$  variable, we need the full covariance matrix between all observables, including all correlations. For example, consider two observables which are correlated and we do not take that into account. If we now compare two different parameter sets and the observables used for the comparison are positively correlated (i.e., one tends to become smaller if the other one does, and vice versa), the parameter sets can look more similar than they actually are. On the contrary, if these observables are anticorrelated, ignoring this correlation would lead us to over-estimate the difference between the compared parameter sets. In fact, including an observable which is strongly (anti)correlated with another observable does not increase the actual amount of information by much, and hence does not significantly improve our chance to discriminate between different sets of parameters.<sup>†</sup> Thus using more observables does not automatically improve the results of a parameter set comparison.

As mentioned in the Introduction, computing the statistical correlation between a large number of kinematical observables constructed from the same set of events is difficult. We therefore use mostly counting observables, with a single kinematical observable per class of events.

The production of the heavier superparticles can trigger quite lengthy decay cascades [1], leading to events with several jets and/or charged leptons. If we classified all events simply by the number (e.g. 0, 1, 2 or 3 and more), charge and flavor of charged leptons we would already have  $4^6 = 4096$  classes of events. If we defined additional sub-classes according to the number of non- $b$ -jets (e.g. 0, 1, 2, 3, or 4 and more) and the number of  $b$ -jets (e.g. 0, 1 or 2 and more) we would end up with  $5 \cdot 3 \cdot 4096 = 61440$  different classes. Even adding a single kinematical observable for each class would double the total number of observables considered. This large number of observables does not seem to be practical. For one thing, our event sample consists of typically 25,000 events after cuts, so most of the classes would be empty.

Instead we consider 84 independent observables. The first one is the total number of events after cuts. Since nearly all parameter sets include a stable neutralino as LSP<sup>‡</sup>, we always require a sizable missing  $E_T$ , which greatly suppresses SM backgrounds. The details of the cuts depend on the number of charged leptons (meaning electrons, muons and tagged hadronically decaying taus), as described in Appendix B. On average around 30% of all supersymmetric

---

<sup>†</sup> In the extreme case there could be a 100% correlation between two (linear combinations of) observables. This would lead to a divergence of the inverse correlation matrix  $V^{-1}$ , because one eigenvalue of  $V$  would be zero. This divergence can be removed by removing one of the observables from the covariance matrix. An actual example of this will be described later in this Section.

<sup>‡</sup> The original parameter sets of [7] include a few examples where the LSP is a slepton, in particular the lighter  $\tilde{\tau}$  eigenstate; even the set of “degenerate pairs” contains such examples. Scenarios with stable or long-lived charged slepton as LSP would be trivial to distinguish from parameter sets where the LSP is a neutralino, using stable charged particle searches. We find that all scenarios where the LSP is not a neutralino can be distinguished from all other scenarios even when only using our standard observables listed below. (In all pairs of parameter sets we compare, at least one LSP is the lightest neutralino).

events pass these cuts and we only consider those events in the following.

We divide the surviving events into twelve mutually exclusive classes depending on the number, charge and flavor of the measured “stable” charged leptons ( $l^\pm = e^\pm$  or  $\mu^\pm$ ;  $\tau$ -leptons decay within the detector and are thus non-trivial to identify experimentally). Note that we only include isolated electrons and muons with pseudorapidity  $|\eta| < 2.5$  and transverse momentum  $p_T > 10$  GeV, as described in Appendix A. 1. The twelve classes of events are:

1.  $0l$ : Events with no charged leptons
2.  $1l^-$ : Events with exactly one charged lepton, with negative charge
3.  $1l^+$ : Events with exactly one charged lepton, with positive charge
4.  $2l^-$ : Events with exactly two charged leptons, with total charge  $-2$  (in units of the proton charge)
5.  $2l^+$ : Events with exactly two charged leptons, with total charge  $+2$
6.  $l_i^+ l_i^-$ : Events with exactly two charged leptons, with opposite charge but the same flavor; i.e.  $e^- e^+$  or  $\mu^+ \mu^-$
7.  $l_i^+ l_j^-$ ;  $j \neq i$ : Events with exactly two charged leptons with opposite charge and different flavor; i.e.  $e^- \mu^+$  or  $e^+ \mu^-$
8.  $l_i^- l_j^- l_j^+$ : Events with exactly three charged leptons with total charge  $-1$ . There is an opposite-charged lepton pair with same flavor. For example  $e^- \mu^- \mu^+$  or  $e^- e^- e^+$
9.  $l_i^+ l_j^+ l_j^-$ : Events with exactly three charged leptons with total charge  $+1$ . There is an opposite-charged lepton pair with same flavor. For example  $e^+ \mu^- \mu^+$  or  $e^+ e^- e^+$
10.  $l_i^- l_j^- l_k^\pm$ ;  $k \neq j, i$  for  $+$ : Events with exactly three charged leptons with total negative charge, i.e. there are at least two negatively charged leptons. There is no opposite-charged lepton pair with same flavor. For example  $e^- e^- \mu^+$  or  $e^- e^- e^-$
11.  $l_i^+ l_j^+ l_k^\pm$ ;  $k \neq j, i$  for  $-$ : Events with exactly three charged leptons with total positive charge, i.e. there are at least two positively charged leptons. There is no opposite-charged lepton pair with same flavor. For example  $e^+ e^+ \mu^-$  or  $e^+ e^+ e^+$
12.  $4l$ : Events with four or more charged leptons

Since we assume first and second generation sleptons to be degenerate, lepton universality will hold for the first and second generation also in the MSSM; there is thus little sense in trying to distinguish between electrons and muons. We do, however, distinguish between positively and negatively charged leptons. Since the initial state at the LHC is not CP self-conjugate, there is no reason to assume that  $l^+$  and  $l^-$  will be produced with equal rate.<sup>§</sup> Moreover, pairs of charged leptons with opposite charge but the same flavor can originate from the decay

---

<sup>§</sup> In the context of the MSSM, squark decays into charginos can yield positive leptons from  $\tilde{u}$  and  $\tilde{d}^*$  decay, and negative leptons from  $\tilde{d}$  and  $\tilde{u}^*$  decays. In the absence of CP violation a sizable charge asymmetry [5] can only result from first generation squarks, since squarks of higher generations will always be created as



of a single neutralino,  $\tilde{\chi}_i^0 \rightarrow l^+ l^- \tilde{\chi}_j^0$  with  $j < i$ ; all other pairs of charged leptons must come from the decays of two different (super)particles. In events containing a pair of oppositely charged leptons it therefore makes sense to distinguish pairs with equal flavor from those with different flavor. However, since events with four or more charged leptons are very rare, we do not attempt to subdivide them any further.

For each of these twelve classes  $c \in \{1, 2, \dots, 12\}$  we save seven observables  $O_{i,c}$ ,  $i \in \{1, 2, \dots, 7\}$ :

- $O_{1,c} = n_c/N$ : The number of events  $n_c$  contained in the given class  $c$  divided by the total number of events  $N$ , i.e. the fraction of all events contained in a given class
- $O_{2,c} = n_{c,\tau^-}/n_c$ : The number of events in a given class  $c$  that contain at least one tagged hadronically decaying  $\tau^-$  divided by the total number of events in this class
- $O_{3,c} = n_{c,\tau^+}/n_c$ : The number of events in a given class  $c$  that contain at least one tagged hadronically decaying  $\tau^+$  divided by the total number of events in this class
- $O_{4,c} = n_{c,b}/n_c$ : The number of events in a given class  $c$  that contain at least one tagged  $b$ -jet divided by the total number of events in this class
- $O_{5,c} = \langle j \rangle_c$ : Average number of non- $b$ -jets of all events within a given class  $c$
- $O_{6,c} = \langle j^2 \rangle_c$ : Average of the square of the number of non- $b$ -jets of all events within a given class  $c$ <sup>¶</sup>
- $O_{7,c} = \langle H_T \rangle_c$ : Average value of  $H_T$  of all events within a given class  $c$ , where  $H_T$  is the scalar sum of the transverse momenta of all hard objects, including the missing  $p_T$

Jets are reconstructed using the anti- $k_T$  scheme of FastJet [13]. They have to satisfy  $p_T > 20$  GeV and  $|\eta| < 4.8$ ;  $b$ -tagging is possible only for jets with  $|\eta| < 2.5$  that contain at least one (decay product of a)  $b$ -flavored hadron.  $\tau$ -leptons can be tagged only if they decay hadronically, are isolated, and their visible decay products satisfy  $p_T > 20$  GeV and  $|\eta| < 2.5$ . The tagging efficiency for taggable  $\tau$ -leptons and  $b$ -jets are each 50 %, i.e. each taggable  $\tau$ -lepton or  $b$ -jet is randomly taken to be tagged or not with 50 % probability. See Appendix A for further details. Since we use only a single kinematical observable for each class, and the classes are all mutually exclusive, we do not have to deal with correlations between different kinematical observables.

Note the difference between observables 2, 3 and 4 on the one hand, and 5 and 6 on the other. The former three observables essentially count all events that contain at least one object of the given type, while the latter count the (square of the) number of jets per event. At least for the parameter sets considered here, the number of events containing a tagged  $\tau$  or  $b$ -jet

---

squark-antisquark pairs. In case of the first generation, essentially only  $SU(2)$  doublet squarks can decay into charginos. The charge asymmetry is therefore obviously sensitive to the difference between the masses of  $\tilde{u}_L$  and  $\tilde{d}_L$  – but these masses are related by  $SU(2)$  invariance [1], and can be taken as equal as far as LHC experiments are concerned. The charge asymmetry will nevertheless be sensitive to the ratio of squark and gluino masses. Moreover, the branching ratios of  $\tilde{u}_L$  and  $\tilde{d}_L$  will have slightly different dependencies on the parameters of the chargino sector.

<sup>¶</sup> If event  $i$  in the given class contains  $N_j^{(i)}$  non- $b$ -jets, then  $\langle j^2 \rangle_c = 1/n_c \sum_{i=1}^{n_c} (N_j^{(i)})^2$ .

is usually small, and the number of events containing two or more such tagged objects is even smaller; it is therefore sufficient to simply count the number of events that contain at least one such object.<sup>||</sup> In contrast, most events do contain several jets. We therefore use two different observables to characterize the distribution in the number of jets in the different event classes.

## 3.2 Covariance Matrix

In order to perform a statistical analysis using these observables we need their full covariance matrix, including all correlations. This subsection contains expressions for all non-vanishing entries of this matrix.

The first observable was the total number of events after cuts,  $N$ ; its variance is simply given by

$$\sigma^2(N) = N. \quad (3.1)$$

The next twelve observables are the fractions of events  $n_c/N$  that belong to each class  $c$ . These twelve observables are not independent, since  $\sum_{c=1}^{12} n_c = N$ , i.e. the fractions add up to unity. This difficulty could be avoided by simply using the twelve  $n_c$  as variables, which are not correlated, and dropping the total number of events  $N$ . The reason why we include  $N$  and the  $n_c/N$  is that we will later assign a much smaller systematical error on the event *fractions*  $n_c/N$  than on the total number of events  $N$ . Note also that the event fractions  $n_c/N$  are not correlated with the total number of events  $N$ , i.e.

$$\text{cov}\left(\frac{n_c}{N}, N\right) = 0 \quad (c \in \{1, 2, \dots, 12\}). \quad (3.2)$$

On the other hand, the covariance between the fraction of events in two different classes  $c$  and  $c'$  is nonzero:

$$\text{cov}\left(\frac{n_c}{N}, \frac{n_{c'}}{N}\right) = \delta_{cc'} \frac{n_c}{N^2} - \frac{n_c n_{c'}}{N^3} \quad (c, c' \in \{1, 2, \dots, 12\}). \quad (3.3)$$

The covariance for identical classes ( $c = c'$ ) equals the variance, i.e. the usual error on the fraction of events in this class. The covariance matrix consisting of the twelve entries constructed according to eq.(3.3) is not invertible, because the rows and columns are linearly dependent. This is a consequence of the constraint  $\sum_c n_c = N$  mentioned above. In fact, it should be clear that it is impossible to create 13 independent observables  $n_c/N$  and  $N$  out of twelve measured event numbers  $n_c$ . The solution of this problem is to exclude one  $n_c/N$  with  $n_c \neq 0$  from our list of observables, and hence from the covariance matrix. So at the end we are left with 84 observables carrying different information instead of 85.

The observables  $O_{2,c} = n_{c,\tau^-}/n_c$ ,  $O_{3,c} = n_{c,\tau^+}/n_c$ ,  $O_{4,c} = n_{c,b}/n_c$  for a class  $c$  have the variances

$$\sigma^2(O_{i,c}) = O_{i,c} \cdot (1 - O_{i,c})/n_c \quad i \in \{2, 3, 4\}. \quad (3.4)$$

---

<sup>||</sup>  $b$ -quarks will nearly always occur in quark-antiquark pairs, but the probability that both members of such pairs are not only taggable, but also tagged is rather low. Also, precisely because  $b$ -quarks almost always occur in pairs distinguishing between events with one or two  $b$ -tags adds additional information only if there is a significant number of events with more than one  $b\bar{b}$  pair in the final state; such events are very rare in our scenarios.

Observables referring to different classes  $c$  are obviously uncorrelated.\*

Within a given class, observable 4 is obviously uncorrelated with observables 2 and 3.  $n_{\tau^-}$  and  $n_{\tau^+}$  have some correlation if there is a sizable fraction of events containing at least one  $\tau^+\tau^-$  pair. In the simple situation where  $\tau$ -leptons can only be produced in such pairs and each  $\tau$ -lepton is identified, the number of events containing (at least) one  $\tau^-$  lepton would obviously be exactly the same as that containing (at least) one  $\tau^+$ . In the more realistic case where a  $\tau$  has a finite (rather small) probability  $p_\tau$  to be tagged, the correlation between  $n_{\tau^-}$  and  $n_{\tau^+}$  scales like  $p_\tau^2$ , while the corresponding diagonal entries of the covariance matrix scale like  $p_\tau$ . Note that  $p_\tau$  includes the geometric acceptance and the hadronic branching ratio of the  $\tau$  in addition to the 50% probability of tagging a taggable  $\tau$ . Moreover, in reality most  $\tau^\pm$  are produced together with an associated  $\tau$ -(anti)neutrino rather than with a second  $\tau^\mp$ , which dilutes the correlation between observables 2 and 3 even further. We therefore ignore the correlation between these observables. We will check the statistical properties of our  $\chi^2$  variable later.

The remaining observables can be written as averages over all events in a given class,  $O_{i,c} = \langle o_i \rangle_c$  with  $o_5 = j$ ,  $o_6 = j^2$ ,  $o_7 = H_T$ . Their variances can be calculated directly from the definition:

$$\sigma^2(O_{i,c}) = \frac{1}{n_c - 1} \cdot (\langle o_i^2 \rangle_c - \langle o_i \rangle_c^2) \quad i \in \{5, 6, 7\}. \quad (3.5)$$

Of these observables, only  $\langle j \rangle_c$  and  $\langle j^2 \rangle_c$  are correlated within a given class:

$$\text{cov}(\langle j \rangle_c, \langle j^2 \rangle_c) = \frac{1}{n_c - 1} \cdot (\langle j^3 \rangle_c - \langle j \rangle_c \langle j^2 \rangle_c). \quad (3.6)$$

Here  $\langle j^3 \rangle_c$  is also determined directly from the (simulated) events.

### 3.3 Test Statistics

Our method of comparing parameter sets is based on an overall  $\chi^2$  variable, defined as:

$$\chi_{AB}^2 = \sum_{m,n} (O_m^A - O_n^B) V_{mn}^{-1} (O_m^A - O_n^B). \quad (3.7)$$

Here  $O_n^A$  is the prediction of parameter set  $A$  for the  $n$ -th observable and  $m, n$  run over all relevant observables. In general the sum in eq.(3.7) therefore includes summation over event classes  $c$  and over the seven kinds of observables  $O_{i,c}$  listed in Subsection 3.1. We will describe later how we determine which observables are relevant for a given comparison; this depends on the parameter sets we are comparing. Finally,  $V^{-1}$  is the inverse of the covariance matrix  $V$  of all relevant observables, with entries

$$V_{ij} = \text{cov}[O_i^A, O_j^A] + \text{cov}[O_i^B, O_j^B]. \quad (3.8)$$

---

\* Note that we are talking about purely statistical correlations here. A fluctuation of events in one class can obviously not affect the number of events in a different, distinct class, nor can it affect the properties of the events in this other class. Different observables may very well be ‘‘physically correlated’’, in that changing the value of some input parameter will lead to simultaneous changes in many observables, including observables in distinct classes. This kind of correlation need not be included when constructing the covariance matrix. It does complicate the estimate of errors on the parameters from an overall  $\chi^2$  fit, which, however, is beyond the scope of this paper.

This corresponds to adding the errors for parameter sets  $A$  and  $B$  in quadrature. The calculation of the covariances for a single parameter set has been described in the previous Subsection.

The main purpose of the present Subsection is to test the statistical properties of our  $\chi^2$  variable. In particular, we want to check that it indeed follows a proper  $\chi^2$  distribution. To that end we interpret eq.(3.7) as if we were comparing two distinct measurements, each with its own statistical uncertainty. We use samples of simulated signal events corresponding to  $10\text{ fb}^{-1}$  of LHC data at  $\sqrt{s} = 14\text{ TeV}$ . We do not include any systematic uncertainties here, since their statistical interpretation is less clear.  $\chi_{AB}^2$  will follow a  $\chi^2$  distribution if the difference between the measurements is entirely due to statistical fluctuations. We therefore compare two different simulations of the *same* parameter sets, but with different seeds of the random number generator.\*

If  $\chi_{AB}^2$  follows a proper  $\chi^2$  distribution, the probability  $p$  of finding a value bigger than the actual one is given by

$$p = \int_{\chi_{AB}^2}^{\infty} f(z, n_d) dz. \quad (3.9)$$

Here

$$f(z, n_d) = \frac{z^{(n_d-2)/2} e^{-z/2}}{2^{n_d/2} \Gamma(n_d/2)} \quad (3.10)$$

is the  $\chi^2$  probability density function and  $n_d$  is the number of degrees of freedom, i.e. the number of observables included in the sum (3.7). Note that eqs.(3.9) and (3.10) assume that  $\chi_{AB}^2$  has been constructed from  $n_d$  Gaussian random variables.

As noted above, we verify the statistical properties of  $\chi_{AB}^2$  by comparing models to themselves. To that end we simulate each model twice, using different seeds in Herwig++. For simplicity we simulate exactly the same number of events in both runs.<sup>†</sup> Each comparison yields a  $p$ -value computed from eqs.(3.9) and (3.10). Performing many such comparisons leads to a distribution of  $p$ -values, which should be flat if  $\chi_{AB}^2$  follows a proper  $\chi^2$  distribution. This is a stringent test of our calculation of the covariance matrix.

In order to achieve higher statistics we use a larger sample of parameter sets than the 384 sets containing the “degenerate pairs” claimed in ref. [7]. Recall that Arkani-Hamed *et. al.* called two parameter sets indistinguishable if their quantity  $(\Delta S_{AB})^2 < 0.285$ . All model pairs with higher values of  $(\Delta S_{AB})^2$  are said to be distinguishable, with the degree of distinguishability

---

\* Strictly speaking a  $\chi^2$  distribution is defined via the sum of the quadratic differences between Gaussian random variables and their means (i.e.,  $\sum_n (O_n - \overline{O_n})^2$ ), not between the members of pairs of Gaussian random variables, divided by the true variance, not by its estimator. However, if both members of the pair of Gaussian random variables whose squared difference we are computing are distributed with the same mean and same variance, a true  $\chi^2$  distribution also results for the sum over the squared differences between the two random variables, provided the variance is increased by a factor of two. The first condition is satisfied since both “data sets” are generated for the same parameter set. The second condition is approximately satisfied since we are normalizing by the total covariance. Of course, replacing the true covariance by its estimator obtained from data is standard practice in physics.

<sup>†</sup> Using a different seed in general also leads to a slightly different estimate of the total sparticle production cross section. Of course, this difference decreases if more events are used to estimate the total cross section; recall that we estimate this cross section from simulations containing 10,000 events, leading to an uncertainty on the cross section from Monte Carlo statistics in the percent range. This is already much smaller than the physical uncertainty of the predicted cross section, e.g. due to missing higher order corrections.

increasing with increasing  $(\Delta S_{AB})^2$ . For the present test we considered all pairs of parameter sets with  $0.285 \leq (\Delta S)^2 < 0.44$ , which are still relatively difficult to distinguish by the criteria of ref. [7]. The upper bound is chosen so that we get a few thousand additional parameter sets, compromising between higher statistics and limited computing power. This sample includes 3305 parameter sets forming in 4654 pairs<sup>‡</sup> in the given range of  $(\Delta S_{AB})^2$ .

We generate two statistically independent data sets for each of these 3305 parameter sets. For each pair of data sets corresponding to a given parameter set we separately look at the total number of events and at the seven kinds of observables defined for each event class; the event classes and observables have been described in Subsection 3.1. When analyzing the total number of events after cuts  $N$  obviously only a single term contributes to the definition of  $\chi_{AB}^2$  in eq.(3.7). In all SUSY scenarios we consider this event number is large enough to use Gaussian statistics. (This will be the case for all conceivable SUSY scenarios, including “no SUSY”, after inclusion of backgrounds.)

In contrast, the remaining observables  $O_{i,c}$  defined in Subsection 3.1 will be approximately Gaussian distributed only if class  $c$  contains a certain minimal number of events. Recall that  $\chi_{AB}^2$  can be expected to follow a  $\chi^2$  distribution only if the observables used in its construction are Gaussian variables. This is true to a good approximation only if sufficiently many events contribute to a given observable.

For example, as already mentioned at the end of Subsection 3.1 the number of events including tagged hadronically decaying  $\tau$ -leptons is in general relatively small. If there is only one identified  $\tau$  event in hundred events of a given class it does not make sense to compare classes containing only ten events, because most of these classes would contain zero or at most one event with an identified  $\tau$ , and Gaussian statistics would not be applicable. This can be seen from the fact that the resulting  $p$ -value from a single comparison of these classes, computed according to eqs.(3.9) and (3.10), would take mostly two discrete values, as can be seen from the following calculation:

$$\begin{aligned}
\chi_{AB}^2 &= \left( \frac{n_{c,\tau^-}^A}{n_{c,A}} - \frac{n_{c,\tau^-}^B}{n_{c,B}} \right)^2 \cdot \left[ \frac{n_{c,\tau^-}^A}{n_{c,A}^2} \cdot \left( 1 - \frac{n_{c,\tau^-}^A}{n_{c,A}} \right) + \frac{n_{c,\tau^-}^B}{n_{c,B}^2} \cdot \left( 1 - \frac{n_{c,\tau^-}^B}{n_{c,B}} \right) \right]^{-1} \\
&\approx \frac{(n_{c,\tau^-}^A - n_{c,\tau^-}^B)^2}{n_{c,A}^2} \cdot \frac{n_{c,A}^2}{n_{c,\tau^-}^A + n_{c,\tau^-}^B} \\
&= \frac{(n_{c,\tau^-}^A - n_{c,\tau^-}^B)^2}{n_{c,\tau^-}^A + n_{c,\tau^-}^B}
\end{aligned} \tag{3.11}$$

Here  $A$  and  $B$  refer to the two data sets, which have been generated using the same parameter set, and  $c$  refers to one of our twelve event classes. The first line follows from eqs.(3.4) and (3.7), and in the second line we used the approximations  $n_{c,A} \approx n_{c,B}$  and  $n_{c,\tau^-}^A, n_{c,\tau^-}^B \ll n_{c,A}$ . The combination  $n_{c,\tau^-}^A = 0, n_{c,\tau^-}^B = 1$  or vice versa thus leads to  $\chi_{AB}^2 \approx 1$ , while  $n_{c,\tau^-}^A = n_{c,\tau^-}^B = 0$  obviously gives  $\chi_{AB}^2 = 0$  for this single observable. Since for small  $n_c$  the observable  $n_{c,\tau^-}$  most likely takes the values 0 or 1, the resulting distribution of  $p$  computed from this one observable would certainly not be flat. Instead, there would be a pronounced peak at  $p = 1$ ,

---

<sup>‡</sup> The given  $(\Delta S)^2$  range actually contains 4658 pairs and 3307 parameter sets, but with two sets problems occurred simulating them with SUSY-HIT followed by Herwig++.

Table 1: The minimal numbers  $n_{i,\min}$  are listed for our seven kinds of observables. For the fraction of all events that belong to a given class,  $n_c/N$ , at least one of the compared data sets  $A$  and  $B$  has to fulfill this condition. For all other observables both data sets have to contain at least  $n_{i,\min}$  events in a given class  $c$  for  $O_{i,c}$  to be included in the calculation of  $\chi_{AB}^2$ .

Observable	$n_{i,\min}$
$n_c/N$	10
$n_{c,\tau^-}/n_c$	500
$n_{c,\tau^+}/n_c$	500
$n_{c,b}/n_c$	50
$\langle j \rangle_c$ and $\langle j^2 \rangle_c$	50
$\langle H_T \rangle_c$	10

since in many pairs of data sets there would be event classes containing no identified  $\tau$ -lepton. Similar remarks apply to the other observables, although we expect more events to contribute non-trivially in these cases.

In the following we therefore require a minimum number of events  $n_{i,\min}$  for a given observable  $O_{i,c}$  to be included in the computation of  $\chi_{AB}^2$ . The values of  $n_{i,\min}$  depend on the kind of observable (labeled by  $i$ ), as listed in Table 1, but are independent of the event class  $c$ . We include  $O_{1,c}$ , the fraction of all events that belong to class  $c$ , in the calculation of  $\chi_{AB}^2$  as long as at least one of the two data sets we are comparing contains  $n_{1,\min} = 10$  or more events; all other observables are only included if both data sets contain at least  $n_{i,\min}$  events. The reason for this is that two data sets are obviously quite different, and hence distinguishable by LHC experiments, if one of them contains many events of a given class, while the second has none or very few such events. Note that the total error will then be dominated by the error on the data set containing many events, and should be (approximately) Gaussian. In contrast, the other observables will have an approximately Gaussian error only if both data sets contain sufficiently many events.

The chosen minimal numbers  $n_{i,\min}$  are shown in Table 1. They were determined by requiring that the distribution of  $p$ -values for a given kind of observable is at least approximately flat. These  $p$ -values have been obtained by collapsing the double sum in eq.(3.7) over the index  $i$  labeling the type of observable to a single term. This allows us to determine the  $n_{i,\min}$  one by one. The choices listed in Table 1 imply that between one and twelve classes of events are used to determine the  $p$ -value for a given kind of observable, depending on the observable and on the input parameters. As expected from our previous discussion,  $n_{2,\min} = n_{3,\min} = 500$  for the fraction of events in a given class containing at least one identified  $\tau^-$  or  $\tau^+$  lepton, respectively, are the highest. For most of the parameter sets we investigate, the bulk of events are in the three classes with at most one lepton; as a result, these three event classes tend to contribute most to the calculation of  $\chi_{AB}^2$  after the conditions summarized in Table 1 are imposed.

We are now ready to show some results of the self-comparison of the 3305 parameter sets considered here. To this end, we show histograms of  $p$ -values computed from eqs.(3.9) and (3.10); each histogram has up to 3305 entries, since exactly two data sets are generated for each set of input parameters. As noted earlier, if  $\chi_{AB}^2$  defined in eq.(3.7) follows a  $\chi^2$  distribution,

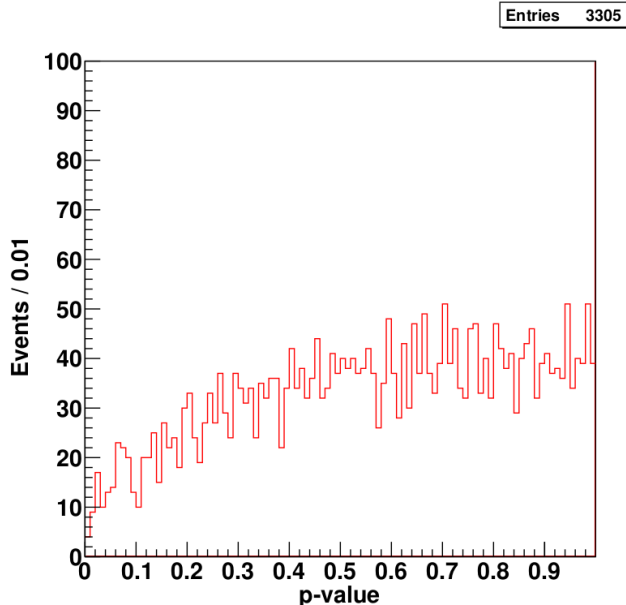


Figure 1: The  $p$ -value distribution of the self-comparison for the sample comprising 3305 parameter sets. Only the total number of events after cuts,  $N$ , is included in the calculation of  $\chi_{AB}^2$  and  $p$ .

these histograms should be (approximately) flat.

Figure 1 shows the distribution of  $p$ -values if only the total number of events after cuts  $N$  is used in the calculation of  $\chi_{AB}^2$ , i.e.,  $n_d = 1$  in eq.(3.10). Evidently this distribution is not flat. The bias towards large  $p$ -values shows that the compared pairs of data sets are more similar than expected if  $N_A$  and  $N_B$  were independent. This is due the fact that for both seeds of the random number generator the same number of events is simulated, which is calculated by multiplying the total cross section for the production of superparticles with the assumed integrated luminosity of  $10 \text{ fb}^{-1}$ . In the absence of cuts we would then always have  $N_A = N_B$ , i.e.  $p = 1$ . In practice the number of accepted events is much smaller than the number of generated events, and the distribution becomes quite flat for  $p \geq 0.4$ . Note that we fix the number of generated events as product of cross section and luminosity also when comparing different sets of input parameters. Strictly speaking, we should instead randomly select the number of generated events from a Poisson distribution whose mean is given by the product of cross section and luminosity. We do not bother to do that since this will not change the statistical distinguishability of two parameter sets significantly. Moreover, simply fixing the number of generated events is conservative, since it tends to reduce  $\chi_{AB}^2$ . Finally, Fig. 1 shows that the distortion of the  $p$ -distribution is not very pronounced, except at very small  $p$ , once cuts have been imposed.

The  $p$ -distributions for the fraction of events containing a reconstructed  $\tau$  are shown in Fig. 2. They follow an overall flat distribution, except for peaks at certain positions. As discussed above, these peaks are caused by the in general low number of events containing identified  $\tau$ -leptons. Since the LHC is a proton-proton collider and therefore has a net positive charge in the final state, fewer hadronically decaying  $\tau^-$  than  $\tau^+$  are identified. Since we use

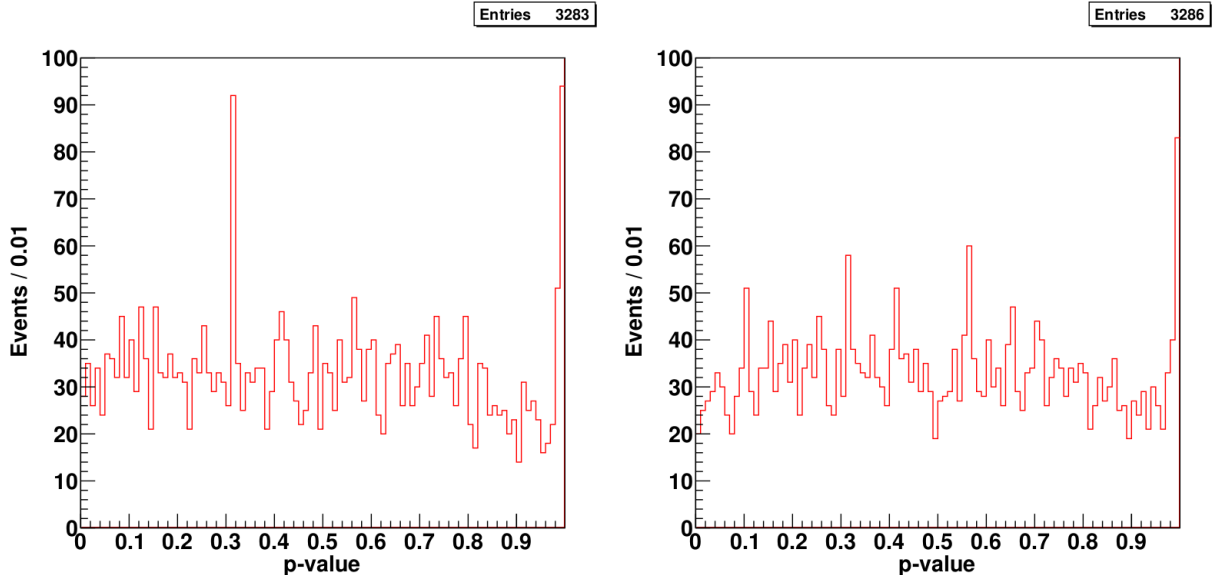


Figure 2: The  $p$ -value distribution of the self-comparison for the sample containing 3305 parameter sets. Only the fraction of events in a given class containing an identified  $\tau^-$  (left) or  $\tau^+$  (right) is included in the calculation of  $p$ . On average 2.8 classes satisfy the requirement  $n_c \geq 500$  (see Table 1) and are thus included in the definition of  $\chi_{AB}^2$ . The number of entries are slightly smaller than 3305 since a pair of data sets for a given set of input parameters is excluded if all variances (of the considered observables) in the compared classes vanish for both data sets or if no class fulfills the  $n_c \geq 500$  requirement.

the same minimal number  $n_{2,\min} = n_{3,\min} = 500$  of required events in a given class for both charges, the peaks are more pronounced for  $\tau^-$  events.

For example, if only a single class contributes to the calculation of  $\chi_{AB}^2$ , and we have exactly one event with an identified  $\tau^-$  in one data set and none in the other, eq.(3.11) gives  $\chi_{AB}^2 \simeq 1$ ; the corresponding  $p$ -value for  $n_d = 1$  compared observable is  $p \approx 0.32$  which is the position of the first peak. Similarly, the peak at  $p = 1$  results from pairs of data sets where each class contains the same number of identified  $\tau$ -leptons of a given charge. This yields  $\chi_{AB}^2 \ll 1^\S$ , and hence  $p \simeq 1$ . Note that pairs of data sets containing not a single identified  $\tau$ -lepton of a given charge in *any* event class are excluded from this comparison since in this case both the numerator and the denominator in our definition (3.7) vanish. Additionally some pairs do not fulfill the  $n_c \geq 500$  requirement for any class. As a result, the numbers of entries in the two frames of Figs. 2 are slightly smaller than 3305. Of course, in this case these observables cannot be included in the calculation of the overall  $\chi_{AB}^2$ , either.

We consider the behavior of the histograms in Fig. 2 acceptable. Having too many pairs of data sets giving a large  $p$ -value, in particular  $p = 1$ , is again conservative. The peak at  $p = 0.32$  probably underestimates the true  $p$ -value for cases where one data set has one identified  $\tau$ -lepton with a given charge and the other has zero<sup>¶</sup>, but not by very much. Note

<sup>§</sup> Eq.(3.11) gives  $\chi_{AB}^2 = 0$  in this case; the exact calculation gives a non-vanishing, but small, value, unless the two values of  $n_c$  also happen to coincide exactly, or  $n_\tau^A = n_\tau^B = 0$ .

<sup>¶</sup> The best estimate of the true expectation value of the number of events with identified  $\tau$ -lepton is then



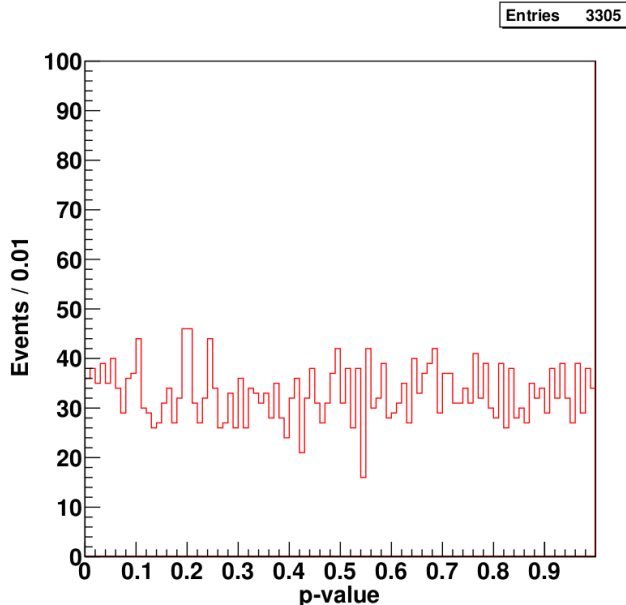


Figure 3: The  $p$ -value distribution of the self-comparison for the sample containing 3305 parameter sets, including all relevant observables. On average around 40 observables are compared for a pair of data sets.

also that these unwarranted peaks are due to data sets containing very few identified  $\tau$ -leptons. In these cases the  $\tau$  observables do not contribute very much to our total  $\chi_{AB}^2$ , and hence do not affect the calculation of the overall  $p$ -value very much.

We checked that the remaining five kinds of observables have flat distributions (not shown) once the conditions summarized in Table 1 have been applied. This justifies our choice of  $n_{i,\min}$  values that define when a given observable is considered relevant.

Finally, in Figure 3 the overall  $p$ -distribution is shown using all types of observables. On average around 40 out of 84 observables are compared for each pair of data sets. The flat shape confirms our calculation method of  $\chi_{AB}^2$ , including the calculation of the covariance matrix as described in Subsection 3.2. It also confirms our expectation that the anomalies we found above in the  $p$ -value distributions for the total number of events after cuts and for the  $\tau$  observables do not distort the overall  $p$ -value significantly.

We also performed a second kind of statistical test, using the 384 parameter sets that contain the indistinguishable pairs found in ref. [7]. We again performed two simulations for each parameter set, one corresponding to the nominal luminosity of  $10\text{fb}^{-1}$ , and one with ten times more events. The first simulation defines the “measurements”, while the second simulation was used to determine the true expectation values of our observables, since their (statistical) errors are much smaller than those of the “measurements”. We then checked whether the normalized differences between the “measurements” and their expectation values follow a Student’s  $t$ -distribution, as they should if the “measured” observables obey Gaussian statistics. These tests were also successful. However, they are somewhat less powerful, since

---

$1/2$ , again ignoring the difference in the numbers of events of the given class between the two data sets. Using Poisson statistics we find that the probability that our  $\chi_{AB}^2 \geq 1$  is then about 0.49.

our computer resources did not permit to generate the required large number of events for the larger number of parameter sets described earlier in this Subsection.

## 4 Results

Having verified that our variable  $\chi_{AB}^2$  behaves like a proper  $\chi^2$  distribution under appropriate conditions, we are now ready to use it to analyze whether pairs of parameter sets can be distinguished by LHC experiments. Our focus will be on pairs of parameter sets that Arkani-Hamed *et al.* [7] deemed to be indistinguishable. Recall that they found 283 such pairs formed from 384 different sets of parameters.

As mentioned in the Introduction, two parameter sets  $A$  and  $B$  can be considered distinguishable if a measurement can exclude the predictions made for parameter set  $B$ , under the assumption that Nature is described by parameter set  $A$ , or vice versa. Here the predictions yield the expectation values of our 84 observables, and do not have a true statistical uncertainty, given sufficiently large Monte Carlo statistics for the computation of these expectation values. Given our limited computer resources, we computed the predictions using ten times more events than generated for the measurement; this ensures that the Monte Carlo statistical uncertainty on the predictions is already almost negligible compared to the expected statistical uncertainty of the measurement, but we do take this uncertainty on the prediction into account.

In most cases it should not make a difference if the experiment is based on parameter set  $A$  while the prediction is for parameter set  $B$  or vice versa. This should only be important if the statistical errors (for fixed integrated luminosity) of  $A$  and  $B$  differ significantly. This can only happen if the predictions for  $A$  and  $B$  are quite different, in which case these parameter sets should be distinguishable anyway. In order to have a unique comparison rule we simply symmetrize the expression for the covariance matrix under the exchange of  $A$  and  $B$ , i.e. we take the average of the covariance matrix that results when measurements based on  $A$  are compared to predictions based on  $B$  and the covariance matrix that describes the difference between measurements based on  $B$  and predictions based on  $A$ :

$$\begin{aligned}
 V_{mn} = & \frac{\text{cov}(O_{m,10}^A, O_{n,10}^A) + \text{cov}(O_{m,10}^B, O_{n,10}^B)}{2} + \frac{\text{cov}(O_{m,100}^A, O_{n,100}^A) + \text{cov}(O_{m,100}^B, O_{n,100}^B)}{2} \\
 & + \delta_{mn} \left( k_m^{(\text{syst})} \frac{O_{m,10}^A + O_{m,10}^B}{2} \right)^2.
 \end{aligned} \tag{4.1}$$

Here the subscripts 10 and 100 refer to data sets corresponding to integrated luminosities of  $10 \text{ fb}^{-1}$  for the measurement and  $100 \text{ fb}^{-1}$  for the prediction.\* The first term in eq.(4.1) therefore describes the (expected) statistical uncertainties associated with the measurements, while the second term comes from the uncertainty on the predictions due to finite (although large) Monte Carlo statistics. Finally, the last term describes systematic uncertainties, which we assume to contribute only to the diagonal elements of the covariance matrix. We assume that the systematic uncertainty for a given observable  $O_m$  is some fixed fraction  $k_m^{(\text{syst})}$  of this observable. This is the usual ansatz at least for systematic theoretical uncertainties; experimental

---

\* Recall that we are predicting the expectation values of our observables. Most of these expectation values are independent of the integrated luminosity. The only exception is the total number of events after cuts, where the prediction obviously is one tenth of the number of accepted events in the larger data sample.

systematic errors also tend to decrease with increasing luminosity. Our numerical choices for the  $k_m^{(\text{syst})}$  will be discussed below.

When calculating the total  $\chi_{AB}^2$  from eq.(3.7), and the corresponding  $p$ -value from eqs.(3.9) and (3.10), we again only include relevant observables, defined exactly as in Subsection 3.3. For the 283 pairs found indistinguishable in ref. [7], we find that on average 32 observables are included in the comparison. Recall that about 40 observables were included in the self-comparison described in the Subsection 3.3. This is expected, since for most observables *both* data sets have to contain a minimal number of events of a given type for a certain observable to be included, as detailed in Table 1. If two different parameter sets are compared it is more likely that one of the sets does not satisfy this criterion, thereby reducing the number of observables we use.

On average about 25,000 events pass all our cuts, for a cut efficiency of about 30%. In most cases a large majority of these events again contains no or only one isolated charged lepton (electron or muon), i.e. the bulk of events belongs to the first three classes described in Subsection 3.1.

In the following three Subsections we present results for four different assumptions regarding systematic errors and Standard Model backgrounds.

## 4.1 No Systematic Errors, no Backgrounds

Our first result is that in an ideal world, where the Standard Model background as well as all systematic errors can be neglected, *all* of the 283 degenerate pairs are distinguishable, i.e. lead to a  $p$ -value below 0.05; the mean  $p$ -value of these 283 pairs is  $6.8 \cdot 10^{-5}$ . Recall that ref. [7] also uses estimated 95% c.l. intervals to define distinguishability.

## 4.2 With Systematic Errors, no Backgrounds

Arkani-Hamed *et al.* did include systematic errors. In order to allow for a direct comparison with their results, we also assume a relatively large systematic uncertainty of 15% on the total number of events after cuts, i.e.  $k_N^{(\text{syst})} = 0.15$ ; this includes the luminosity error on the experimental side, and the uncertainty in the prediction of the total cross section on the theory side. Again following ref. [7] we assign much smaller systematic errors of 1%, i.e.  $k_m^{(\text{syst})} = 0.01$ , to all other observables. This inclusion of systematic uncertainties does not change the criteria defining which observables are included in the comparison. After these systematic uncertainties are included, 260 of the pairs deemed indistinguishable by Arkani-Hamed *et al.* still have  $p$ -values below 0.05, i.e. can be distinguished. We find that only 23 pairs have  $p > 0.05$ , which increases the mean  $p$ -value to 0.038. Note that most pairs have very small  $p$ -values. For example, only 51 pairs have  $p > 10^{-4}$ .

In order to interpret the distribution of  $p$ -values we consider the quantity  $(\Delta P_{AB})^2$  introduced by Arkani-Hamed *et al.*, which is defined by

$$(\Delta P_{AB})^2 = \frac{1}{n_{para}} \sum_{i=1}^{n_{para}} \left( \frac{P_i^A - P_i^B}{\bar{P}_i^{AB}} \right)^2 . \quad (4.2)$$

Here  $P_i^A$  and  $P_i^B$  are the values of the  $i$ -th parameter for parameter sets  $A$  and  $B$ , respectively, and  $n_{para} \leq 15$  is the number of parameters used in a given comparison.  $\bar{P}_i^{AB} = (P_i^A + P_i^B)/2$

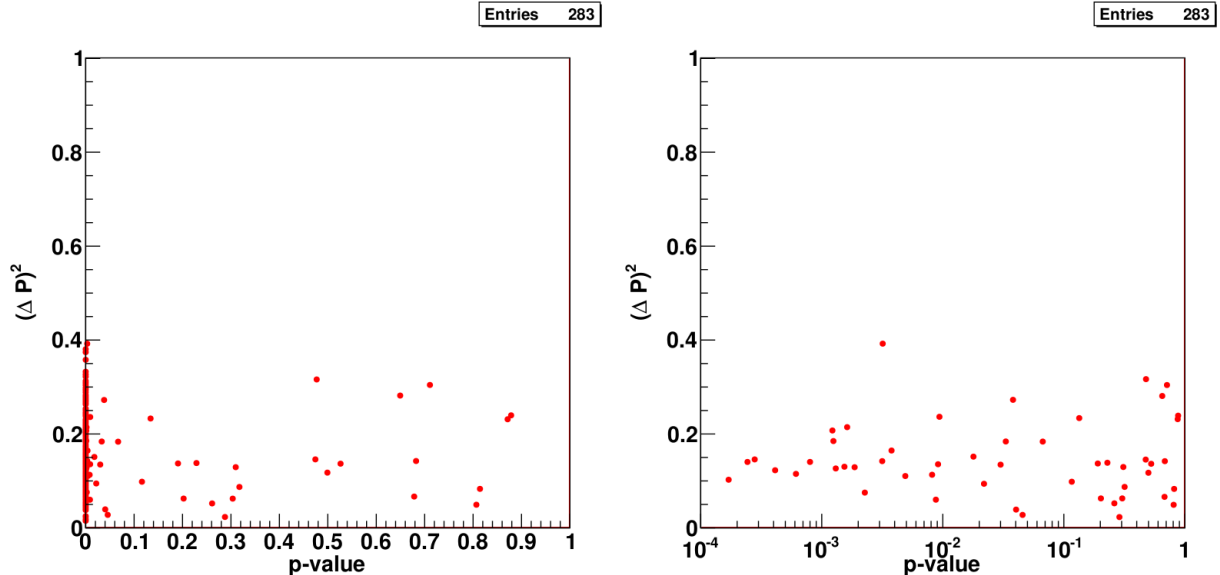


Figure 4: The total parameter difference  $(\Delta P)^2$  defined in eq.(4.2) including all 15 parameters versus the  $p$ -value for the 283 pairs deemed indistinguishable in ref. [7], including systematic errors. The  $p$ -value is shown on a linear (left) and logarithmic scale (right); in the latter case pairs with  $p < 10^{-4}$  are not shown.

is the average value of the  $i$ -th parameter for both sets. Since all our parameters are positive,  $(\Delta P_{AB})^2$  can take values in the range  $[0, 4]$ . For small values it corresponds approximately to the relative difference squared, i.e.  $(\Delta P_{AB})^2 = 0.01$  implies a 10% difference between the parameters of the parameter sets  $A$  and  $B$ .

Clearly in the limit  $(\Delta P_{AB})^2 \rightarrow 0$  the two parameter sets  $A$  and  $B$  become identical, and hence indistinguishable. One could naively expect that pairs of parameter sets giving a large value of  $(\Delta P_{AB})^2$  should be relatively easy to distinguish. However, in Fig. 4 we see that is not necessarily the case: there are pairs of parameter sets where *both*  $(\Delta P_{AB})^2$  and the  $p$ -value are quite large. This indicates that, at least under certain circumstances, the observables we are considering are not sensitive to some of our parameters. We remind the readers that all our parameter sets have relatively light superparticles, not much above the TeV scale, so the total rate of SUSY events is significant. Recall also that *all* pairs of parameter sets we are considering here were considered indistinguishable by Arkani-Hamed et al., including parameter sets with relatively large  $(\Delta P_{AB})^2$ . As noted above, our analysis shows that most of these pairs can in fact be distinguished.

In the right frame of Fig. 4, which uses a logarithmic scale for the  $p$ -value, the lower edge of the populated region includes smaller  $(\Delta P_{AB})^2$  for larger  $p$ -values, which conforms with naive expectations. However, in the left frame, which uses a linear  $x$ -axis and includes all 283 pairs, we also find some pairs where both  $(\Delta P_{AB})^2$  and  $p$  are quite small. This can e.g. happen if a small variation of some mass opens or closes some decay channel characterized by large couplings and hence potentially large branching ratios, which will significantly alter the final state of many SUSY events. The main conclusion therefore is that there is relatively little correlation between the  $p$ -value and the average parameter difference  $(\Delta P_{AB})^2$  computed from

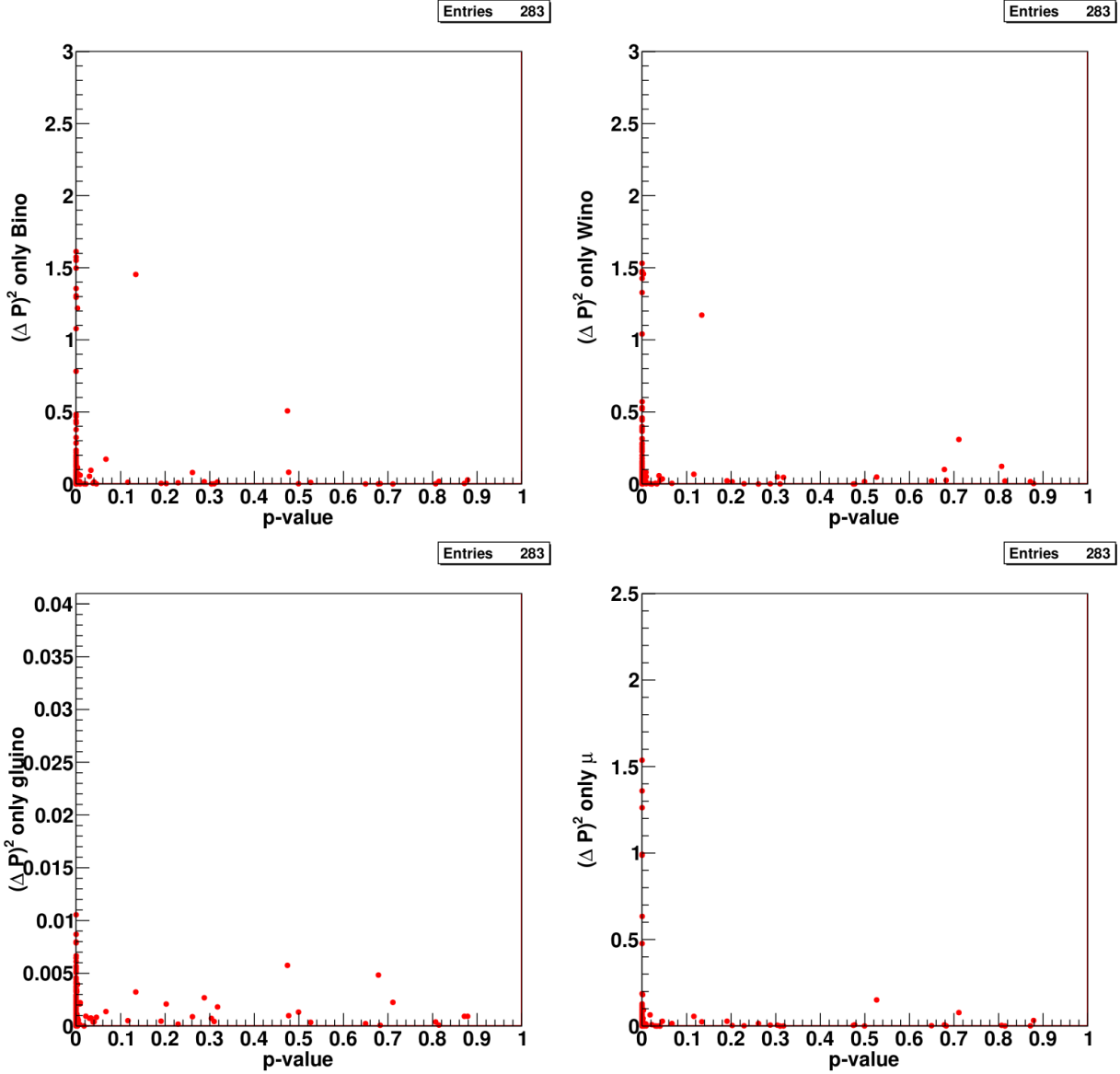


Figure 5: As in Fig. 4, except that only a single parameter has been used in the calculation of  $(\Delta P)^2$ :  $M_1$  (top left),  $M_2$  (top right),  $M_3$  (bottom left),  $\mu$  (bottom right).

all 15 input parameters.

In order to gain a better understanding of this result, we consider results where only a subset of our 15 free parameters has been used in the calculation of  $(\Delta P_{AB})^2$ . We begin with Fig. 5, which shows results where  $(\Delta P_{AB})^2$  has been calculated from a single parameter in the gaugino–higgsino sector. We see that pairs of parameter sets that have  $p > 0.05$  have gluino masses that differ by at most 7%. This is not surprising since, given our assumption  $|M_3| \lesssim 1$  TeV, a significant change of the gluino mass inevitably leads to a significant change of the total number of SUSY events.

Among the parameters in the electroweak gaugino–higgsino sector,  $\mu$  shows the smallest difference between pairs of parameter sets with  $p > 0.05$ , with  $(\delta\mu_{AB})^2 \lesssim 0.15$ ; this is to be

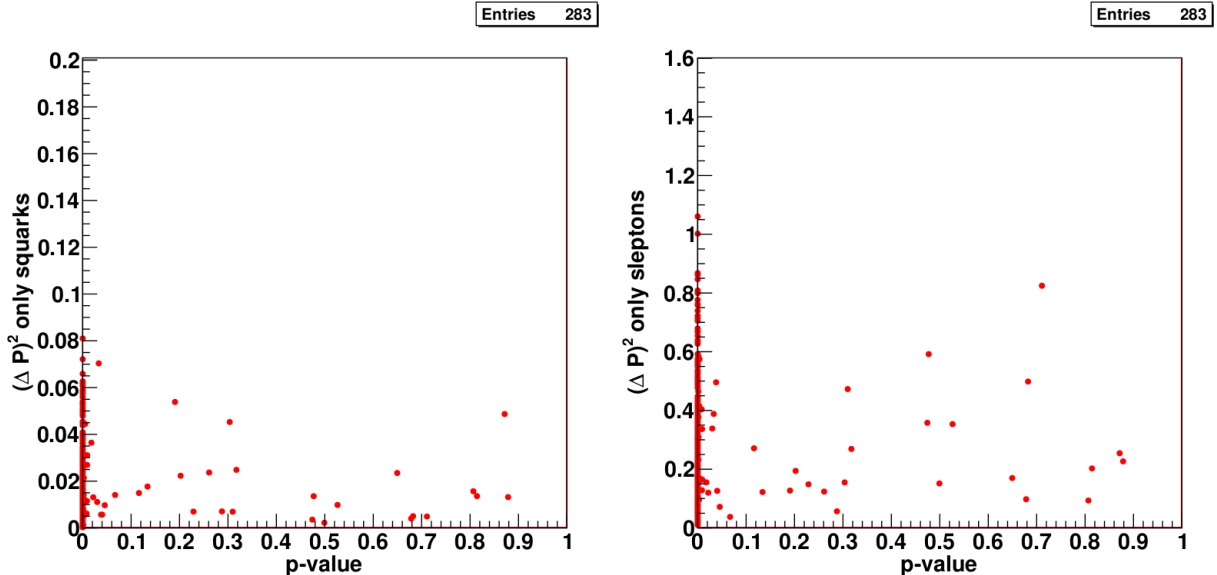


Figure 6: As in Fig. 4, except that the calculation of  $(\Delta P)^2$  includes only the squark (left) or the slepton mass parameters (right).

contrasted with  $(\delta\mu_{AB})^2 \lesssim 1.5$  if all pairs considered indistinguishable in ref. [7] are considered. The fact that  $\mu$  shows the smallest difference in pairs that are difficult to distinguish can be understood from the observation that this parameter not only largely determines the masses of two neutralinos and one chargino, but also affects mixing among third generation sfermions. A change of  $\mu$  therefore generally changes more observables than changes of the electroweak gaugino mass parameters  $M_1$  and  $M_2$  do.

Most pairs of parameter sets with  $p > 0.05$  also have quite similar values of these latter parameters, but there are a few outliers. This is due to the fact that our counting observables are mostly sensitive to the ordering of the three electroweak gaugino–higgsino mass parameters. For example, reducing the smallest of these parameters even more may have little impact on branching ratios, and may not change our sole kinematic quantity  $H_T$  very much as long as the lightest neutralino remains sufficiently light. Conversely, if the bino mass is larger than the gluino mass and also larger than the masses of the sleptons, few bino–like neutralinos will be produced at the LHC, so that  $|M_1|$  cannot be determined very well by LHC experiments.

The two points with  $p \approx 0.13$  and  $(\Delta P_{AB})^2 > 1$  in the two upper frames of Fig. 5 correspond to the same pair of parameters. Here the values of  $M_1$  and  $M_2$  are (approximately) interchanged between the two sets. The existence of such “mirror pairs” has also been noticed in ref. [7]. Note that there is a strong hierarchy between these two parameters in both cases; moreover,  $\mu$  is quite large. As a result, basically only the lightest neutralino is produced in LHC events, irrespective of the ordering of  $M_1$  and  $M_2$ . In the scenario with  $M_2 \ll M_1$ , the lightest chargino is also produced frequently; however, since its mass splitting to the lightest neutralino is only  $\mathcal{O}(100)$  MeV, the lighter chargino effectively behaves like the lightest neutralino in this scenario, as far as our observables are concerned.

Figure 6 shows results for sfermion mass parameters. In the left frame the sum in eq.(4.2) runs over the six squark mass parameters of our model. We see that the squark masses differ

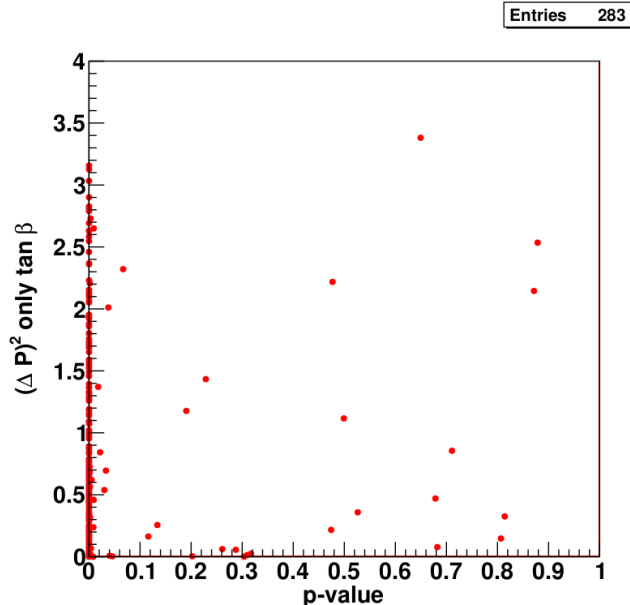


Figure 7: As in Fig. 4, except that  $(\Delta P)^2$  is calculated only from  $\tan\beta$ .

relatively little within pairs of parameter sets with  $p > 0.05$ , although the spread is significantly larger than for the gluino mass (up to about 24 % as compared to up to about 7 %). The reason is that the cross section for producing a single type of squark is much smaller than the cross section for gluino pair production, for equal masses; this is true in particular for second and third generation squarks, for which no  $t$ - or  $u$ -channel processes involving two valence ( $u$  or  $d$ ) quarks in the initial state are available. Moreover, one can again set up “mirror pairs”, e.g. by swapping the masses of  $SU(2)$  doublet ( $L$ -type) and singlet ( $R$ -type) squarks if all squarks decay directly into the lightest neutralino.

The right frame of Fig. 6 shows corresponding results for the slepton mass parameters. Evidently parameter pairs with  $p > 0.05$  can have quite different slepton masses. The observables we are using are sensitive to slepton masses essentially only if sleptons are produced in the decays of strongly interacting sparticles. While the conditions (2.1) make it likely that such decays are kinematically possible for some strongly interacting sparticle(s), they by no means ensure that the corresponding cross section times branching ratio is sizable. In particular, we saw above that bino-like neutralinos may be produced very rarely at the LHC. If in addition the wino-like states are lighter than the sleptons, very few sleptons will be produced in the decays of gluinos and squarks, and our observables will not be sensitive to slepton masses.

Finally, Fig. 7 shows that  $\tan\beta$  has the largest spread among all our parameters, even when only pairs of parameter sets with  $p > 0.05$  are considered. In principle this parameter has influence on many observables, since it appears in the chargino and neutralino mass matrices and also affects all sfermion masses. However, in most cases the dependence of the physical masses and couplings on this parameter is weak. It can be enhanced if two charginos or two neutralinos are close in mass, or if  $\tan\beta$  is very large, in which case it modifies  $\tilde{b}$  and  $\tilde{\tau}$  mixing significantly.

### 4.3 Including Standard Model Background

We next include Standard Model backgrounds, which had been ignored in ref. [7]. We include backgrounds from  $Z + \text{jets}$ ,  $W + \text{jets}$  and  $t\bar{t}$  as well as single top production; the latter is generated using the programs MadGraph 5 [14] and Herwig++, and the other backgrounds are simulated directly using Herwig++. For the first two backgrounds, only leptonic  $W$  and  $Z$  decays are included, which have a chance to pass our cut on the missing transverse momentum.<sup>†</sup> All background (and signal) contributions are only considered to leading order in perturbation theory.

Altogether we find 29,052 background events after cuts for a data sample of  $10 \text{ fb}^{-1}$ , yielding a signal to background ratio of very roughly 1 to 1. We add these to all our “measurement” samples. An independent background simulation for  $100 \text{ fb}^{-1}$  of data yielded 293,875 events after cuts, which we add to our “prediction” samples. The biggest source of background is top pair production, followed by the production of a  $W$  or  $Z$  boson in association with several jets. Of course, the background is also included in the calculation of the covariance matrix.

Recall that a given observable is only included in the calculation of the overall  $\chi_{AB}^2$  if the corresponding event class contains a minimal number of signal events, as listed in Table 1. We now demand instead that there should be a SUSY signal of at least  $3\sigma$  statistical significance for an observable to be considered relevant, i.e. we only include observables if the number of supersymmetric events in the corresponding class is greater or equal three times the square-root of the number of background events.<sup>‡</sup> In case of the event fractions in a given event class  $O_{1,c}$ , this requirement has to be satisfied for at least one of the two pairs of parameters in a given comparison; all other observables are included only if this new requirement is satisfied for both pairs of parameters.

Including these backgrounds, but ignoring all systematic errors leads to only one parameter pair with  $p > 0.05$ . However, including systematic errors as well as SM backgrounds increases the number of pairs that cannot be distinguished “at 95% confidence level” to 46. This means that our simple algorithm can resolve more than 80% of the “degenerate pairs” found by Arkani-Hamed et al., even after SM backgrounds are included.

## 5 Summary and Conclusions

In this paper we investigated the question to which extent a single  $\chi^2$  variable can be used to discriminate between different parameter sets in a general MSSM with 15 free parameters. This analysis was triggered by ref. [7], which identified 283 pairs of parameter sets that were claimed to be indistinguishable by LHC experiments with  $10 \text{ fb}^{-1}$  of data taken at  $\sqrt{s} = 14 \text{ TeV}$ . In our analysis we used far fewer observables (up to 84, as compared to up to 1808), but took care to properly include all correlations, so that our  $\chi_{AB}^2$  defined in eq.(3.7) should behave like a proper  $\chi^2$  distribution in the limit of Gaussian statistics; we checked this explicitly in Sec. 3.3. We saw

---

<sup>†</sup> In order to reduce the number of generated events we require a minimum transverse momentum of the  $Z$  and  $W$ , respectively, of  $100 \text{ GeV}$  at the parton level, i.e. prior to showering. This has little influence on the total number of events which pass the cuts because events with lower parton-level transverse momentum have almost no chance to pass our missing  $p_T$  cut.

<sup>‡</sup> The analogous requirement on our first observable, the total number of events after cuts, is satisfied for all scenarios we are considering.



Table 2: Number of pairs of parameter sets with  $p > 0.05$ , out of the 283 pairs deemed indistinguishable in ref. [7], for different levels of sophistication of our analysis (with or without systematic errors and Standard Model backgrounds). The mean and median values of  $p$  for all 283 pairs are also given.

Syst. Errors	Backgrounds	no. of pairs with $p > 0.05$	$\bar{p}$	median $p$
No	No	0	$6.8 \cdot 10^{-5}$	$3.6 \cdot 10^{-146}$
Yes	No	23	0.038	$1.1 \cdot 10^{-36}$
No	Yes	1	0.0030	$2.6 \cdot 10^{-79}$
Yes	Yes	46	0.079	$1.4 \cdot 10^{-13}$

in the Introduction that this does not seem to be true for the “ $\chi^2$ -like” variable considered in ref. [7]. We also improved the analysis by including initial state showering and the underlying event when simulating our signal events. We also analyzed the effects of Standard Model backgrounds.

Our results are summarized in Table 2. We see that under the conditions of ref. [7] (with systematic errors but without backgrounds) all but 23 of the supposedly 283 indistinguishable pairs of parameters can in fact be distinguished at the 95% confidence level. The median  $p$ -value for all 283 pairs is then of order  $10^{-36}$ . Including also SM backgrounds increases the number of pairs with  $p > 0.05$  to 46, and the median  $p$ -value increases by a factor  $10^{23}$  – but it still remains very small, of order  $10^{-13}$ . We therefore conclude that our analysis strategy can greatly alleviate the “inverse problem” at the LHC.

This Table also indicates that the inclusion of systematic uncertainties has a bigger impact than the inclusion of SM backgrounds. This is somewhat worrisome, since our ansatz for the systematic errors is quite ad hoc. Experimental systematic errors can only be estimated properly by our experimental colleagues. The rather small total systematic errors we include can only be realized once quantum corrections to all relevant cross sections and branching ratios have been computed. We are confident that this will happen if and when superparticles are discovered; in this we are encouraged by a very recent NNLO calculation of the cross section for  $t\bar{t}$  production from  $q\bar{q}$  annihilation [15], which reduces the higher order uncertainty, estimated by varying unphysical factorization and renormalization scales, to a value below 3%. Recall also that all sparticles have masses at or below 1 TeV in the parameter sets considered in ref. [7], leading to quite large event samples at the LHC; this reduces the importance of backgrounds. As noted earlier, many of these spectra are most likely excluded by existing LHC searches; we nevertheless used them in our analysis to ensure that our results can be compared directly with those of ref. [7].

While we consider our results to be quite encouraging, we saw in Sec. 4.2 that in some cases our observables cannot discriminate between sets where at least some of the input parameters differ quite significantly, even if backgrounds are ignored. The pairs with  $p > 0.05$  and the largest overall difference between input parameters, measured via the quantity  $(\Delta P_{AB})^2$  introduced in eq.(4.2), all have squark and gluino masses near the upper end of the scanned range, i.e. relatively low sparticle production cross sections and hence relatively small event samples. Moreover, they all have wino mass  $M_2 \ll |\mu|, |M_1|$ , i.e. a light wino-like lightest chargino with small mass splitting to the neutralino. In fact, the mass splitting is  $\lesssim 200$  MeV, giving

macroscopic decay length for the lightest chargino [16]. A measurement of this decay length would give an additional constraint on our input parameters. For example, it would break the degeneracy between pairs that basically only differ by  $M_1 \leftrightarrow M_2$ ; see the discussion of Fig. 5.

Similarly, we have not tried to isolate certain supersymmetric production channels. Our cuts have been devised solely with the purpose of suppressing SM backgrounds; no attempt has been made to suppress “supersymmetric backgrounds” to certain channels. For example, direct slepton pair production might be detectable at the LHC under certain circumstances [17]. This should help to resolve at least some of our degeneracies.

Note also that our simulation does not include mixed  $\mathcal{O}(\alpha_S\alpha_W)$  contributions to squark production cross sections, which are mostly due to interference between QCD diagrams and diagrams where an electroweak gaugino is exchanged in the  $t$ - or  $u$ -channel. These contributions can change some squark pair cross sections by tens of percent [18], thereby offering another handle on the electroweak gaugino masses; they can also help to discriminate between  $SU(2)$  singlet and doublet squarks, which can be difficult if only a single neutralino state is accessible to squark and gluino decays.

Finally, we have not seriously attempted to optimize the cuts, or the selection of observables, with a view of improve the distinguishability between pairs of parameter sets. We feel that this can be done in a meaningful manner only if many more than the 283 pairs of parameter sets we are studying are analyzed, which unfortunately is beyond the power of our computer resources. Besides, given that the LHC is running and producing data, the usefulness of vast scans of parameter space for the purpose of optimizing methods to distinguish between discrete sets of input parameters appears somewhat questionable.

Instead the analysis presented here had two objectives. First, we wanted to alleviate concerns raised in ref. [7] that LHC experiments may not be able to determine many SUSY parameters even if sparticles are quite light. As argued above, this goal was largely achieved. This indicates that our observables should also be useful for determining the values of supersymmetric parameters, rather than “only” for the purpose of discriminating between discrete sets of input parameters. Our second goal is therefore to motivate further studies, where (some of) our observables are used to determine supersymmetric parameters, as alternative, or in addition, to the methods that have been used so far.

## Acknowledgments

We thank Jesse Thaler for providing the parameter sets analyzed by us. NB wants to thank the “Bonn-Cologne Graduate School of Physics and Astronomy” and the “Universität Bonn” for the financial support. This work was partially supported by the BMBF–Theorieverbund and by the Helmholtz Alliance “Physics at the Terascale”.

## A Definition of Observables

In this Appendix we describe in detail how our observables are defined. In particular, charged leptons and jets have to fulfill certain acceptance cuts to be counted. The  $\tau$ -jets which arise from hadronically decaying  $\tau$ -leptons are in general just called taus here. The determination of  $b$ - and non- $b$ -jets is also explained in the following. The final subsections deal with the

calculation of the missing transverse momentum  $\cancel{p}_T$  and the observable  $H_T$ .

Note that we count visible particles as measurable only if they have pseudorapidity  $|\eta| < 5$ ; neutrinos and the lightest neutralino are not considered visible, since they (usually) do not interact in the detector.

## A.1 Electrons and Muons

We only consider *isolated* electrons and muons, i.e. a charged lepton  $l$  has to fulfill the following criteria:

- $|\eta^l| < 2.5$
- $p_T^l > 10 \text{ GeV}$
- For all measurable particles with  $\Delta R = \sqrt{(\eta^l - \eta)^2 + (\phi^l - \phi)^2} \leq 0.2$  the transverse energy  $E_T$  is summed. This sum has to be  $\sum E_T < 5 \text{ GeV}$

## A.2 Taus

Only hadronically decaying taus, i.e.  $\tau$ -jets, are considered here; the electrons and muons produced in leptonic  $\tau$  decays are counted as all other charged leptons, if they satisfy the criteria listed in the previous Subsection. We use generator information to check whether a given  $\tau$ -lepton indeed decays hadronically. The four-momentum  $p^\tau$  of the  $\tau$ -jet is then defined as the difference between the four-momentum of the parent  $\tau$ -lepton and the four-momentum of the corresponding  $\nu_\tau$ . We impose the following acceptance cuts on the  $\tau$ -jets:

- $|\eta^\tau| < 2.5$
- $p_T^\tau > 20 \text{ GeV}$

Furthermore the  $\tau$ -jet should be isolated, i.e. there must not be any charged hadrons with  $p_T > 1 \text{ GeV}$  and no photons with  $p_T > 1.5 \text{ GeV}$  within a cone  $\Delta R = \sqrt{(\eta^\tau - \eta)^2 + (\phi^\tau - \phi)^2} < 0.5$  around the tau; note that this condition is usually more stringent than that used for electrons and muons. Moreover, a  $\tau$ -jet satisfying all conditions is only tagged with a 50 % probability. Recall also that some 35 % of all  $\tau$ -leptons decay leptonically. Altogether we thus see that a sample of events containing equal numbers of electrons, muons and  $\tau$ -leptons with identical kinematical distributions would indeed yield equal numbers of observed electrons and muons in our simulation, but far fewer identified  $\tau$ -leptons. Note finally that identified  $\tau$ -jets are not included in the identification of other jets.

## A.3 Jets

Jets are determined with the program FastJet [13] using the anti- $k_t$  algorithm. All measurable particles are taken into account, except for isolated electrons and muons that satisfy the criteria of Subsec. A.1 as well as isolated  $\tau$ -jets defined in Subsec. A.2. We use the following parameter choices for the jet finding algorithm:

- double dou\_R = 0.5

- `fastjet::RecombinationScheme RecSch_scheme = fastjet::E_scheme`
  - `fastjet::Strategy Stra_strategy = fastjet::Best`
- `fastjet::JetDefinition JetDef_def(JetAlgo_algo, dou_R, RecSch_scheme, Stra_strategy)`

Reconstructed jets are only counted if they satisfy:

- $p_T^j > 20 \text{ GeV}$
- $|\eta^j| < 4.8$

In order to determine whether a given jet originates from a  $b$ -quark, we first check the progenitors of all particles in the jet (except for the photons). All particles that originate from the decay of one of the  $b$ -hadrons  $B^0$ ,  $\bar{B}^0$ ,  $B^+$ ,  $B^-$ ,  $B_s^0$ ,  $\bar{B}_s^0$ ,  $\Lambda_b^0$  or  $\bar{\Lambda}_b^0$  are marked. If a jet contains at least one such particle and the pseudorapidity fulfills  $|\eta^{b\text{-jet}}| < 2.5$  then the jet is identified as a  $b$ -jet at the generator level. Note that the number of  $b$ -jets could differ from the number of decaying  $b$ -hadrons already at this stage. In particular, the products of multiple  $b$ -hadrons could end up in one jet, which is not unlikely if the two corresponding  $b$ -quark momenta are nearly parallel to each other. In principle the decay products of one  $b$ -hadron could end up in multiple jets, but this happens only rarely. Finally, a  $b$ -jet is only tagged with a 50% probability. All jets which are not tagged as  $b$ -jets are counted as non- $b$ -jets. Note that we ignore the possibility that jets which do not originate from a  $b$ -quark are tagged as  $b$ -jets (false positive tags).

## A.4 Missing Transverse Momentum

In the simulation the transverse momentum vectors of all measurable particles are added. The missing transverse momentum  $\vec{p}_T$  is the negative of this sum,  $\vec{p}_T = -\sum_i \vec{p}_{i,T}$ . Our event selection includes a cut on the absolute value of this quantity,  $p_T = |\vec{p}_T|$ .

## A.5 $H_T$

$H_T$  is defined as the sum of the transverse momenta of all hard objects and the absolute value of the missing  $p_T$ . Hard objects are all isolated leptons and jets that satisfy the criteria outlined above.

# B Selection Cuts

As well known, the production of heavy superparticles can be detected at the LHC on top of SM backgrounds only after cuts have been applied to reduce these backgrounds. We apply three different sets of selection cuts, depending on the number and charge of identified leptons. Note that we include identified  $\tau$ -jets as leptons for the purpose of defining these cuts. In the following we outline cuts for events with at most one lepton, events with exactly two opposite-charged leptons, and events containing at least two leptons of the same charge (and possibly some additional lepton(s) of arbitrary charge). All leptons and jets have to satisfy the criteria described in Appendix A.

## B.1 Events with at Most One Lepton

We impose the following cuts:

- $\cancel{p}_T > 200$  GeV
- $H_T > 1000$  GeV

Additionally there are either exactly two or at least four jets, on which we apply the following cuts:

### B.1.1 Two Jets

This event sample will get contributions from squark pair production if at least one squark decays directly to the lightest neutralino (possibly plus very soft particles).

- $E_T^j > 300, 150$  GeV for the hardest and second-hardest jet
- There are no additional jets with transverse energy  $E_T^j > 30$  GeV and no  $b$ -jets; this is intended to reduce backgrounds from top production
- $m^{jj} > 200$  GeV
- If there is exactly one lepton then its transverse mass with the missing transverse momentum in the event should fulfill  $m_T(\vec{p}^l, \vec{\cancel{p}}_T) > 80$  GeV; this suppresses backgrounds where the missing  $p_T$  comes from  $W^\pm \rightarrow l^\pm \nu_l$  decays. This event sample will get contributions from squark pair production where exactly one squark decays into a chargino which in turn decays leptonically.

### B.1.2 Four or More Jets

This event sample will get contributions from gluino pair production, and from squark production in the presence of long decay chains and/or additional QCD radiation.

- $E_T^j > 100, 50, 50, 50$  GeV for the four hardest jets
- Find the smallest invariant mass of two of the four hardest jets,  $m_{\min}^{jj}$  (there are six combinations). Find the smallest invariant mass of three of the four jets,  $m_{\min}^{3j}$  (there are four combinations). At least one of the following three requirements has to be fulfilled, in order to suppress  $t\bar{t}$  backgrounds:
  - Either:  $m_{\min}^{jj} > 100$  GeV
  - Or:  $m_{\min}^{3j} > 200$  GeV
  - Or: None of the four jets is a  $b$ -jet
- If there is exactly one lepton then its transverse mass with the missing transverse momentum in the event should fulfill  $m_T(\vec{p}^l, \vec{\cancel{p}}_T) > 80$  GeV; this again suppresses backgrounds where the missing  $p_T$  originates from a  $W$  decay

## B.2 Events with Two Opposite-Charged Leptons

We impose the following cuts:

- $\cancel{p}_T > 100$  GeV
- If the two leptons are an  $e^+e^-$  or a  $\mu^+\mu^-$  pair their invariant mass should satisfy one of the following requirements, which will remove events where the leptons come from a  $Z \rightarrow l^+l^-$  decay:

Either:  $m^{ll} \leq 75$  GeV

Or:  $m^{ll} \geq 105$  GeV

In addition, we demand that the event contains either no, at least three or at least four jets; in the latter two cases we apply additional cuts in order to suppress the  $t\bar{t}$  background:

### B.2.1 No Jets

- There are no jets with  $E_T^j > 30$  GeV

### B.2.2 Three or More Jets

- There are at least three jets with  $E_T^j > 100, 100, 50$  GeV
- None of the three highest  $E_T^j$  jets has been tagged as a  $b$ -jet

### B.2.3 Four or More Jets

- There are at least four jets, with  $E_T^j > 100, 50, 50, 50$  GeV

## B.3 Events with at least Two Leptons of the Same Charge

We impose the following cuts:

- $\cancel{p}_T > 50$  GeV
- $\cancel{p}_T > 3 \cdot \sqrt{H_T}$  (in GeV). This is intended to suppress events where the missing  $p_T$  is due to mismeasurements; for example it is not unlikely to find 1 TeV measured energy accompanied by more than 50 GeV missing transverse momentum
- Now consider all lepton pairs with opposite charge but same flavor, i.e.  $e^+e^-$ ,  $\mu^+\mu^-$  or  $\tau^+\tau^-$ . If there is *no* such lepton pair, the event is accepted. Otherwise we impose the following two additional cuts:

If the event contains exactly three charged leptons, define the third lepton  $l_3$  as the one *not* counted in the opposite-charged same-flavored lepton pair. The event then has to satisfy  $m_T(\vec{p}_{l_3}, \vec{\cancel{p}}_T) > 80$  GeV. If all three leptons are of the same flavor, there are two possible  $l^+l^-$  pairs, and hence two possible choices for  $l_3$ ; in this case this last cut has to be satisfied for both choices.

In addition, each  $l^+l^-$  pair must be an  $e^+e^-$  or  $\mu^+\mu^-$  pair with invariant mass below 75 GeV or above 105 GeV (to suppress  $Z \rightarrow l^+l^-$  backgrounds), or the event must contain at least two jets with  $E_T^j > 100$ , 100 GeV

## References

- [1] For introductions to supersymmetry, see M. Drees, R.M. Godbole and P. Roy, “Theory and Phenomenology of Sparticles”, World Scientific, Singapore (2004); H.A. Baer and X.R. Tata, “Weak scale supersymmetry: From superfields to scattering events”, Cambridge University Press (2006).
- [2] I. Hinchliffe, F.E. Paige, M.D. Shapiro, J. Soderqvist and W. Yao, *Phys. Rev.* **D55**, 5520 (1997) [hep-ph/9610544]; H. Bachacou, I. Hinchliffe and F.E. Paige, *Phys. Rev.* **D62**, 015009 (2000) [hep-ph/9907518]; I. Hinchliffe and F.E. Paige, *Phys. Rev.* **D61**, 095011 (2000) [hep-ph/9907519]; B.C. Allanach, C.G. Lester, M.A. Parker and B.R. Webber *JHEP* **0009**, 004 (2000) [hep-ph/0007009]; M. Drees et al., *Phys. Rev.* **D63**, 035008 (2001) [hep-ph/0007202]; J. Hisano, K. Kawagoe and M.M. Nojiri, *Phys. Rev.* **D68**, 035007 (2003) [hep-ph/0304214]; K. Kawagoe, M.M. Nojiri and G. Polesello, *Phys. Rev.* **D71**, 035008 (2005) [hep-ph/0410160]; G.G. Ross and M. Serna, *Phys. Lett.* **B665**, 212 (2008) [arXiv:0712.0943 [hep-ph]]; M.M. Nojiri, G. Polesello and D. Tovey, *JHEP* **0805**, 014 (2008) [arXiv:0712.2718 [hep-ph]]; N. Kersting, *Phys. Rev.* **D79** (2009) 095018 [arXiv:0901.2765 [hep-ph]]; D. Costanzo and D.R. Tovey, *JHEP* **0904** (2009) 084 [arXiv:0902.2331 [hep-ph]]; M. Burns, K.T. Matchev and M. Park, *JHEP* **0905** (2009) 094 [arXiv:0903.4371 [hep-ph]]; H.-C. Cheng, J.F. Gunion, Z. Han and B. McElrath, *Phys. Rev.* **D80** (2009) 035020 [arXiv:0905.1344 [hep-ph]]; K.T. Matchev, F. Moortgat, L. Pape and M. Park, *JHEP* **0908** (2009) 104 [arXiv:0906.2417 [hep-ph]]; B. Webber, *JHEP* **0909** (2009) 124 [arXiv:0907.5307 [hep-ph]]; K.T. Matchev, F. Moortgat, L. Pape and M. Park, *Phys. Rev.* **D82** (2010) 077701 [arXiv:0909.4300 [hep-ph]]; V. Barger, Y. Gao, A. Lessa and X. Tata, *Phys. Rev.* **D83** (2011) 095013 [arXiv:1103.0018 [hep-ph]]; H. -C. Cheng and J. Gu, *JHEP* **1110** (2011) 094 [arXiv:1109.3471 [hep-ph]]; B. Dutta, T. Kamon, A. Krislock, K. Sinha and K. Wang, arXiv:1112.3966 [hep-ph].
- [3] C.G. Lester and D.J. Summers, *Phys. Lett.* **B463**, 99 (1999) [hep-ph/9906349]; C. Lester and A. Barr, *JHEP* **0712**, 102 (2007) [arXiv:0708.1028 [hep-ph]]; B. Gripaios, *JHEP* **0802**, 053 (2008) [arXiv:0709.2740 [hep-ph]]; A.J. Barr, B. Gripaios and C.G. Lester, *JHEP* **0802**, 014 (2008) [arXiv:0711.4008 [hep-ph]]; W.S. Cho, K. Choi, Y.G. Kim and C.B. Park, *Phys. Rev. Lett.* **100**, 171801 (2008) [arXiv:0709.0288 [hep-ph]], and *JHEP* **0802**, 035 (2008), [arXiv:0711.4526 [hep-ph]]; M.M. Nojiri, Y. Shimizu, S. Okada and K. Kawagoe, *JHEP* **0806**, 035 (2008) [arXiv:0802.2412 [hep-ph]]; D.R. Tovey, *JHEP* **0804**, 034 (2008) [arXiv:0802.2879 [hep-ph]]; A.J. Barr, G.G. Ross and M. Serna, *Phys. Rev.* **D78** 056006 (2008) [arXiv:0806.3224 [hep-ph]]; M.M. Nojiri, K. Sakurai, Y. Shimizu and M. Takeuchi, *JHEP* **0810**, 100 (2008) [arXiv:0808.1094 [hep-ph]]; H. -C. Cheng and Z. Han, *JHEP* **0812** (2008) 063 [arXiv:0810.5178 [hep-ph]]; M. Burns, K. Kong, K.T. Matchev and M. Park, *JHEP* **0810**, 081 (2008) [arXiv:0808.2472 [hep-ph]], and [arXiv:0810.5576 [hep-ph]]; A. J. Barr, A. Pinder and M. Serna, *Phys. Rev.* **D79**

- (2009) 074005 [arXiv:0811.2138 [hep-ph]]; T. Han, I.-W. Kim and J. Song, *Phys. Lett.* **B693** (2010) 575 [arXiv:0906.5009 [hep-ph]]; A.J. Barr, B. Gripaios and C.G. Lester, *JHEP* **0911** (2009) 096 [arXiv:0908.3779 [hep-ph]]; G. Polesello and D.R. Tovey, *JHEP* **1003** (2010) 030 [arXiv:0910.0174 [hep-ph]]; I. -W. Kim, *Phys. Rev. Lett.* **104** (2010) 081601 [arXiv:0910.1149 [hep-ph]]; K.T. Matchev and M. Park, *Phys. Rev. Lett.* **107** (2011) 061801 [arXiv:0910.1584 [hep-ph]]; P. Konar, K. Kong, K.T. Matchev and M. Park, *JHEP* **1004** (2010) 086 [arXiv:0911.4126 [hep-ph]]; T. Cohen, E. Kuffik and K.M. Zurek, *JHEP* **1011** (2010) 008 [arXiv:1003.2204 [hep-ph]]; C.G. Lester, *JHEP* **1105** (2011) 076 [arXiv:1103.5682 [hep-ph]]; A.J. Barr et al., *Phys. Rev.* **D84** (2011) 095031 [arXiv:1105.2977 [hep-ph]]; K. Choi, D. Guadagnoli and C. B. Park, *JHEP* **1111** (2011) 117 [arXiv:1109.2201 [hep-ph]]; P. Baringer, K. Kong, M. McCaskey and D. Noonan, *JHEP* **1110** (2011) 101 [arXiv:1109.1563 [hep-ph]]; D. Curtin, *Phys. Rev.* **D85** (2012) 075004 [arXiv:1112.1095 [hep-ph]].
- [4] H. Baer, X. Tata and J. Woodside, *Phys. Rev.* **D45**, 142 (1992); H. Baer, M. Drees, C. Kao, M.M. Nojiri and X. Tata, *Phys. Rev.* **D50**, 2148 (1994) [hep-ph/9403307]; D. Feldman, Z. Liu and P. Nath, *Phys. Rev. Lett.* **99**, 251802 (2007), Erratum-ibid. **100**, 069902 (2008) [arXiv:0707.1873 [hep-ph]], and *JHEP* **0804**, 054 (2008) [arXiv:0802.4085 [hep-ph]]; M. Drees, J.M. Kim and E.-K. Park, *Phys. Rev.* **D82** (2010) 095005 [arXiv:1006.2100 [hep-ph]].
- [5] H. Baer, C.-h. Chen, F. Paige and X. Tata, *Phys. Rev.* **D53** (1996) 6241 [hep-ph/9512383].
- [6] C.G. Lester, M.A. Parker and M.J. White, 2, *JHEP* **0601** (2006) 080 [hep-ph/0508143]; H.K. Dreiner, M. Krämer, J.M. Lindert and B. O’Leary, *JHEP* **1004** (2010) 109 [arXiv:1003.2648 [hep-ph]]; J.A. Conley, H.K. Dreiner L. Glaser, M. Krämer and J. Tattersall, *JHEP* **1203** (2012) 042 [arXiv:1110.1287 [hep-ph]].
- [7] N. Arkani-Hamed, G.L. Kane, J. Thaler and L.-T. Wang, *JHEP* **0608**, 070 (2006) [hep-ph/0512190].
- [8] ATLAS collab., G. Aad *et al.*, *Phys. Rev. Lett.* **106** (2011) 131802 [arXiv:1102.2357 [hep-ex]]; *Phys. Lett.* **B701** (2011) 186 [arXiv:1102.5290 [hep-ex]]; *Phys. Lett.* **B701** (2011) 398 [arXiv:1103.4344 [hep-ex]]; *Eur. Phys. J.* **C71** (2011) 1682 [arXiv:1103.6214 [hep-ex]]; *Phys. Lett.* **B710** (2012) 67 [arXiv:1109.6572 [hep-ex]]; *Phys. Rev.* **D85** (2012) 012006 [arXiv:1109.6606 [hep-ex]]; *Phys. Lett.* **B709** (2012) 137 [arXiv:1110.6189 [hep-ex]]; *Eur. Phys. J.* **C72** (2012) 1993 [arXiv:1202.4847 [hep-ex]]; arXiv:1203.5763 [hep-ex]; arXiv:1203.6193 [hep-ex]; arXiv:1204.3852 [hep-ex]; arXiv:1204.5638 [hep-ex]; and arXiv:1204.6736 [hep-ex]; CMS collab., S. Chatrchyan *et al.*, *Phys. Lett.* **B698** (2011) 196 [arXiv:1101.1628 [hep-ex]]; *JHEP* **1107** (2011) 113 [arXiv:1106.3272 [hep-ex]]; *JHEP* **1108** (2011) 156 [arXiv:1107.1870 [hep-ex]]; and *Phys. Rev. Lett.* **107** (2011) 221804 [arXiv:1109.2352 [hep-ex]].
- [9] B.C. Allanach, *Comput. Phys. Commun.* **143** (2002) 305 [hep-ph/0104145].
- [10] A. Djouadi, M. Mühlleitner and M. Spira, *Acta Phys. Polon.* **B38** (2007) 635 [hep-ph/0609292].



- [11] M. Bähr *et. al.*, *Eur. Phys. J.* **C58** (2008) 639 [arXiv:0803.0883 [hep-ph]].
- [12] P. M. Nadolsky *et. al.*, *Phys. Rev.* **D78** (2008) 013004 [arXiv:0802.0007 [hep-ph]].
- [13] M. Cacciari, G.P. Salam and G. Soyez, *Eur. Phys. J.* **C72** (2012) 1896 [arXiv:1111.6097 [hep-ph]].
- [14] J. Alwall *et. al.*, *JHEP* **1106**, 128 (2011), [arXiv:1106.0522 [hep-ph]]
- [15] P. Baernreuther, M. Czakon and A. Mitov, arXiv:1204.5201 [hep-ph].
- [16] C.-H. Chen, M. Drees and J.F. Gunion, *Phys. Rev.* **D55** (1997) 330, Erratum-ibid. **D60** (1999) 039901 [hep-ph/9607421].
- [17] F. del Aguila and L. Ametller, *Phys. Lett.* **B261** (1991) 326; H. Baer, C.-h. Chen, F. Paige and X. Tata, *Phys. Rev.* **D49** (1994) 3283 [hep-ph/9311248]; Yu.M. Andreev, S.I. Bitjukov and N.V. Krasnikov, *Phys. Atom. Nucl.* **68** (2005) 340 [hep-ph/0402229]
- [18] S. Bornhauser, M. Drees, H.K. Dreiner and J.S. Kim, *Phys. Rev.* **D76** (2007) 095020 [arXiv:0709.2544 [hep-ph]].